

Signal Temporal Logic Control Synthesis among Uncontrollable Dynamic Agents with Conformal Prediction

Xinyi Yu, Yiqi Zhao, Xiang Yin, and Lars Lindemann *

October 15, 2024

Abstract

The control of dynamical systems under temporal logic specifications among uncontrollable dynamic agents is challenging due to the agents' a-priori unknown behavior. Existing works have considered the problem where either all agents are controllable, the agent models are deterministic and known, or no safety guarantees are provided. We propose a predictive control synthesis framework that guarantees, with high probability, the satisfaction of signal temporal logic (STL) tasks that are defined over a controllable system in the presence of uncontrollable stochastic agents. We use trajectory predictors and conformal prediction to construct probabilistic prediction regions for each uncontrollable agent that are valid over multiple future time steps. Specifically, we construct a normalized prediction region over all agents and time steps to reduce conservatism and increase data efficiency. We then formulate a worst-case bilevel mixed integer program (MIP) that accounts for all agent realizations within the prediction region to obtain an open-loop controller that provably guarantee task satisfaction with high probability. To efficiently solve this bilevel MIP, we propose an equivalent MIP program based on KKT conditions of the original bilevel formulation. Building upon this, we design a closed-loop controller, where both recursive feasibility and task satisfaction can be guaranteed with high probability. We illustrate our control synthesis framework on two case studies.

1 Introduction

Consider the following scenarios in which autonomous dynamical systems need to operate safely among uncontrollable dynamical agents: mobile service robots operating in pedestrian-rich environments, self-driving cars navigating through dense urban traffic, and leader-follower systems such as truck platoons reducing air drag to improve fuel economy. All these scenarios have in common that the autonomous system needs to satisfy complex safety-critical specifications in the presence of uncontrollable agents. Achieving these specifications is challenged by the fact that communication is prohibited, limited and unstable, or only one-directional, while the agents' intentions may not always be known. In this setting, the autonomous system needs to make predictions about the behavior of the dynamic agents and select safe actions accordingly. In this work, we propose a predictive control synthesis framework with probabilistic safety for complex temporal logic specifications.

Control of multi-agent systems under temporal logic specifications has attracted much attention, see e.g., [1–8]. However, the agent dynamics here are usually known and agents are assumed to be

*Xinyi Yu, Yiqi Zhao and Lars Lindemann are with Thomas Lord Department of Computer Science, University of Southern California, Los Angeles, CA 90089, USA. e-mail: {xinyi.yu12, yiqizhao, llindema}@usc.edu. Xiang Yin is with Department of Automation and Key Laboratory of System Control and Information Processing, Shanghai Jiao Tong University, Shanghai 200240, China. e-mail: yinxiang@sjtu.edu.cn.

collaborative. In this paper, we are interested in control synthesis among uncontrollable dynamic stochastic agents under temporal logic tasks, and specifically in settings where communication is limited and no information about agent intentions and models is available. This problem has been studied in the literature, e.g., using sampling-based approaches [9, 10], game theory [11], supervisory control theory [12], or optimization-based methods [13–15]. These works, however, only consider qualitative temporal logic specifications such as linear temporal logic, while we are here interested in quantitative temporal logics that allow to measure the quality of task satisfaction. More importantly, these works make simplifying assumptions on the models of the agents such as being linear or having Gaussian noise distributions. Recent works in [16–19] make no such assumptions and instead use learning-enabled trajectory predictors and conformal prediction to obtain probabilistic prediction regions that can be used for downstream control. However, these works do not consider complex specifications expressed in temporal logics. Note that extending the control frameworks aforementioned to the temporal logic case is not straightforward, since temporal logic specifications are defined over agent trajectories while the aforementioned works only consider point-wise state constraints (see more discussions at the end of section 2.1).

Contribution. We consider the signal temporal logic (STL) control synthesis problem in the presence of uncontrollable dynamic agents without making any assumptions on the agents’ dynamics and distribution. Specifically, we make the following contributions:

- We use trajectory predictors and conformal prediction to construct probabilistic prediction regions that contain the trajectories of multiple uncontrollable agents.
- We propose a new mixed integer program (MIP) based on a worst case formulation of the STL constraints over all uncontrollable agent trajectories within these prediction regions. We present an equivalent MIP program based on KKT conditions of the original MIP to efficiently compute the open-loop controller that provably guarantee task satisfaction with high probability.
- To obtain a closed-loop controller, we introduce a recursively feasible model predictive control (MPC) framework, where recursive feasibility through the task horizon can be guaranteed with high probability. We again guarantee task satisfaction with high probability.
- We validate and illustrate the efficacy of our algorithms on temperature control and robot motion planning problems.

Organization. After discussing related work in Section 1.1, we present preliminaries and the problem definition in Section 2. We show how to compute prediction regions for multiple uncontrollable agents using conformal prediction in Section 3 and present predictive STL open-loop and closed-loop control synthesis frameworks in Section 4 and 5, respectively. We present simulations in Section 6 and conclude in Section 7.

1.1 Related Work

Quantitative temporal logics such as signal temporal logic (STL) [20] have increasingly been used in control. The reason for their success in control is their ability to reason over the robustness of a control system with respect to the specification via the STL quantitative semantics [21, 22]. The quantitative semantics of STL provide a natural control objective that can be maximized, e.g., via gradient-based optimization [23–26], mixed integer programming [27–29], or control barrier functions [30–32].

While STL control synthesis problems have been well studied for deterministic systems, the problem becomes more challenging for stochastic systems. There are various approaches that

ensure probabilistic task satisfaction, e.g., via mixed integer programming [33–35], sampling-based approaches [36–38], and stochastic control barrier functions [39]. Another recent line of work considers the minimization of mathematical risk of STL specifications [40–42]. In addition, there are also some related approaches for reactive STL control synthesis, see e.g., [43–46].

Conceptually closest to our work are [16, 17, 19] where the authors apply conformal prediction to obtain probabilistic prediction regions of uncontrollable dynamic stochastic agents. Conformal prediction is a lightweight statistical tool for uncertainty quantification, originally introduced in [47, 48], that has recently attracted attention within the machine learning community, see e.g., [49, 50] for up-to-date tutorials. Compared to [16, 17, 19], we consider complex signal temporal logic specifications, that are defined over agent trajectories as opposed to considering simple state constraints. Previous works hence do not apply to our settings as we have to account for state couplings at different times. Furthermore, complex temporal logic tasks require the data-efficient computation of non-conservative probabilistic prediction regions to promote long horizon control with multiple agents. We therefore propose an efficient method for computing prediction regions, and then formulate a robust control problem which is fundamentally different and less conservative from Lipschitz-based formulations proposed in the aforementioned works.

2 Preliminaries & Problem Definition

We consider an autonomous system, e.g., a robotic system or an autonomous car, that is described by the discrete-time dynamics

$$x_{k+1} = f(x_k, u_k), \quad x_0 \in \mathcal{X} \quad (1)$$

where the function $f : \mathcal{X} \times \mathcal{U} \rightarrow \mathcal{X}$ is defined over the state and input domains \mathcal{X} and \mathcal{U} , respectively. Here, x_0 is the known initial state and $x_k \in \mathcal{X} \subset \mathbb{R}^{n_x}$ and $u_k \in \mathcal{U} \subset \mathbb{R}^m$ are the n_x -dimensional state and the m -dimensional control input at time k , respectively. To synthesize control sequences later, let us also define $\mathbf{u}_{k:T-1} := u_k \dots u_{T-1}$ and $\mathbf{x}_{k+1:T} := x_{k+1} \dots x_T$.

The system in equation (1) operates among N uncontrollable and stochastic dynamic agents, e.g., autonomous or remote-controlled robots or humans. We model the state of agent i at time k as a random variable $Y_{k,i} \in \mathcal{Y}_i \subset \mathbb{R}^{n_{y,i}}$ with state domain \mathcal{Y}_i , and we define the random state of all agents as $Y_k := [Y_{k,1}, \dots, Y_{k,N}] \in \mathcal{Y} \subset \mathbb{R}^{n_y}$ with $n_y := n_{y,1} + \dots + n_{y,N}$ and $\mathcal{Y} := \mathcal{Y}_1 \times \dots \times \mathcal{Y}_N$. We do not assume to have any a-priori knowledge of the agent dynamics and intentions, and since the agents are uncontrollable, their finite-length trajectories are a-priori unknown. However, we assume that their trajectories follow an unknown distribution \mathcal{D} , i.e.,

$$Y := (Y_0, Y_1, \dots) \sim \mathcal{D}.$$

We further assume that we have access to \bar{K} realizations from \mathcal{D} .

Assumption 1 *We have access to \bar{K} independent trajectories $Y^{(j)} := (Y_1^{(j)}, Y_2^{(j)}, \dots)$ from the distribution \mathcal{D} . We split the trajectories into calibration and training sets $D_{cal} := \{Y^{(1)}, \dots, Y^{(K)}\}$ and $D_{train} := \{Y^{(K+1)}, \dots, Y^{(\bar{K})}\}$, respectively.*

Modeling dynamic agents by a distribution \mathcal{D} includes general classes of systems such as discrete-time stochastic hybrid systems and Markov decision processes. We make the restriction that \mathcal{D} does not depend on the behavior of the autonomous system in (1), i.e., \mathcal{D} does not depend on x . Similar modeling assumptions have been made in [16] and are justified in many applications, e.g., when conservative control actions are taken in autonomous driving that do only alter the

behavior of pedestrians minimally. By using robust or adaptive versions of conformal prediction, see e.g., [51, 52], we can relax this assumption. Lastly, Assumption 1 is not restrictive in most applications, e.g., past trajectory data of dynamic agents is available in robotic or transportation systems.

In this paper, we consider the control of the system in (1) under temporal logic specifications that are jointly defined over the system and the uncontrollable agents. Therefore, we define their joint state at time k as $S_k := [x_k, Y_k] \in \mathcal{X} \times \mathcal{Y} \subset \mathbb{R}^n$ with $n := n_x + n_y$ and the joint state sequence as $\mathbf{S} := S_0, S_1, \dots$

2.1 Signal Temporal Logic Control Synthesis among Uncontrollable Agents

In this paper, we use signal temporal logic to describe the tasks defined over the system in (1) and uncontrollable agents. Signal temporal logic was originally introduced in [20], and we here only give a brief introduction. The syntax of discrete-time finite-length STL formulae is

$$\phi ::= \top \mid \pi^\mu \mid \neg\phi \mid \phi_1 \wedge \phi_2 \mid \phi_1 \mathbf{U}_{[a,b]} \phi_2, \quad (2)$$

where \top is the true symbol (\perp denotes the false symbol) and $\pi^\mu : \mathbb{R}^n \rightarrow \{\top, \perp\}$ is a predicate whose truth value is determined by the sign of an underlying predicate function $\mu : \mathbb{R}^n \rightarrow \mathbb{R}$, i.e., for the state $s \in \mathbb{R}^n$ we have that $\pi^\mu(s) := \top$ if and only if $\mu(s) \geq 0$. The symbols \neg and \wedge denote the standard Boolean operators “negation” and “conjunction”, respectively, and $\mathbf{U}_{[a,b]}$ is the temporal operator “until” with $a \leq b$, $a, b \in \mathbb{N}$ with \mathbb{N} being the natural numbers. As we consider a discrete-time setting, we use $[a, b]$ to denote the discrete-time interval $[a, b] \cap \mathbb{N}$. These operators can be used to define “disjunction” by $\phi_1 \vee \phi_2 := \neg(\neg\phi_1 \wedge \neg\phi_2)$, “implication” by $\phi_1 \rightarrow \phi_2 := \neg\phi_1 \vee \phi_2$, “eventually” by $\mathbf{F}_{[a,b]}\phi := \top \mathbf{U}_{[a,b]}\phi$, and “always” by $\mathbf{G}_{[a,b]}\phi := \neg \mathbf{F}_{[a,b]}\neg\phi$.

STL Semantics. STL formulae are evaluated over trajectories $\mathbf{s} := s_0 s_1 \dots$ where \mathbf{s} could be a realization of \mathbf{S} . The notation $(\mathbf{s}, k) \models \phi$ denotes that \mathbf{s} satisfies the STL formula ϕ at time k . Particularly, we have $(\mathbf{s}, k) \models \pi^\mu$ iff $\mu(s_k) \geq 0$, $(\mathbf{s}, k) \models \neg\phi$ iff $(\mathbf{s}, k) \not\models \phi$, $(\mathbf{s}, k) \models \phi_1 \wedge \phi_2$ iff $(\mathbf{s}, k) \models \phi_1$ and $(\mathbf{s}, k) \models \phi_2$, and $(\mathbf{s}, k) \models \phi_1 \mathbf{U}_{[a,b]}\phi_2$ iff $\exists k' \in [k+a, k+b]$ such that $(\mathbf{s}, k') \models \phi_2$ and $\forall k'' \in [k, k']$, we have $(\mathbf{s}, k'') \models \phi_1$, i.e., ϕ_2 will hold some time between $[k+a, k+b]$ in the future and until then ϕ_1 always holds. We write $\mathbf{s} \models \phi$ instead of $(\mathbf{s}, 0) \models \phi$ for simplicity.

STL Quantitative Semantics. In addition to these *qualitative* Boolean semantics, we can also define *quantitative* semantics $\rho^\phi(\mathbf{s}, k) \in \mathbb{R}$, also referred to as robust semantics, that describe how well ϕ is satisfied [53]. Formally, we have

$$\begin{aligned} \rho^\top(\mathbf{s}, k) &:= \infty \\ \rho^{\pi^\mu}(\mathbf{s}, k) &:= \mu(s_k) \\ \rho^{\neg\phi}(\mathbf{s}, k) &:= -\rho^\phi(\mathbf{s}, k) \\ \rho^{\phi_1 \wedge \phi_2}(\mathbf{s}, k) &:= \min(\rho^{\phi_1}(\mathbf{s}, k), \rho^{\phi_2}(\mathbf{s}, k)) \\ \rho^{\phi_1 \mathbf{U}_{[a,b]}\phi_2}(\mathbf{s}, k) &:= \max_{k' \in [k+a, k+b]} \min(\rho^{\phi_2}(\mathbf{s}, k'), \min_{k'' \in [k, k']} \rho^{\phi_1}(\mathbf{s}, k'')). \end{aligned}$$

Problem Formulation. In this paper, we consider bounded STL formulae ϕ where time intervals $[a, b]$ in ϕ are bounded. The satisfaction of a bounded STL formula ϕ can be computed over bounded trajectories. Specifically, we require trajectories with a minimum length of T_ϕ where T_ϕ is the formula horizon formally defined in [54, 55]. For example, for $\phi := \mathbf{F}_{[3,8]}\mathbf{G}_{[1,2]}\pi^\mu$, we have $T_\phi = 10$. We additionally assume that ϕ is in positive normal form, i.e., the formula ϕ contains no negations, and is build from convex and differentiable predicate functions μ . The former assumption

is without loss of generality as every STL formula can be re-written into an equivalent STL formula that is in positive normal form [28, 55]. The latter assumption is made for computational reasons and can be relaxed, since every STL formula can be transformed into positive normal form (see [55] for more details). We summarize these assumptions next.

Assumption 2 *We consider bounded STL formulae ϕ in positive normal form. We further assume that all predicate functions μ in ϕ are convex and differentiable with respect to Y_τ .*

We impose specifications ϕ that satisfy Assumption 2 over the random trajectory \mathbf{S} , i.e., over the system trajectory x_k and the random trajectories of uncontrollable dynamic agents Y_k . Formally, we consider the following problem in this paper.

Problem 1 *Given the system in (1), the uncontrollable agents $Y := (Y_0, Y_1, \dots) \sim \mathcal{D}$, a set of trajectories D_{cal} and D_{train} that satisfy Assumption 1, an STL formula ϕ from (2) that satisfies Assumption 2, and a failure probability $\delta \in (0, 1)$, compute the control inputs u_k for all $k \in \{0, \dots, T_\phi - 1\}$ such that the STL formula is satisfied with a probability of at least $1 - \delta$, i.e.,*

$$Prob(\mathbf{S} \models \phi) \geq 1 - \delta.$$

The challenge for solving Problem 1 is the dependency of ϕ on the agents in Y , i.e., the joint trajectory \mathbf{S} is only partially controllable. Therefore, our approach is to predict uncontrollable agents, construct prediction regions that capture uncertainty of these prediction, and synthesize the controller using this information. While our work is inspired by [16, 17], these works cannot be simply extended to solve our problem, since they consider state constraints of the form $c(x_k, y_k) \geq 0$ that are enforced at each time step separately. We instead consider STL specifications defined over the trajectory \mathbf{S} , where the task description cannot be separated into different time steps. This temporal coupling makes the problem of designing closed-loop controllers different from existing works, since during the online execution we cannot discard constraints from previous time steps. Furthermore, applying a Lipschitz reformulation to this problem as in [16, 17] will bring conservative results. Specifically, these works leverage the Lipschitz constant of the function c to capture the worst case over the prediction region. In the STL case, taking the Lipschitz constant of the robustness function ρ^ϕ may be conservative and not practical.

2.2 Trajectory Predictors and Conformal Prediction

Trajectory Predictors. From the training set D_{train} , we first train a trajectory predictor that estimates future states $(Y_{k+1}, \dots, Y_{T_\phi})$ from past observations (Y_0, \dots, Y_k) . Specifically, we denote the predictions made at time k as $(\hat{Y}_{k+1|k}, \dots, \hat{Y}_{T_\phi|k})$. For instance, we can use recurrent neural networks (RNNs) [56], long short term memory (LSTM) networks [57], or transformers [58]. In this paper, we do not make assumption on the trajectory predictor.

Conformal Prediction. The predictions $\hat{Y}_{\tau|k}$ of Y_τ for $\tau > k$, which may be obtained from learning-enabled components, may not always be accurate. We will use conformal prediction to obtain prediction regions for Y_τ that are valid with high probability. We leverage conformal prediction which is a statistical tool for uncertainty quantification with minimal assumptions [47, 48].

Let $R^{(0)}, \dots, R^{(K)} \in \mathbb{R}$ be $K + 1$ i.i.d. random variables which are referred to as the *nonconformity score*. For instance, we may define the prediction error $R^{(j)} := \|Y_\tau^{(j)} - \hat{Y}_{\tau|k}^{(j)}\|$ at time $\tau > k$ for all calibration trajectories $Y^{(j)} \in D_{cal}$. Naturally, a small value of $R^{(j)}$ in this case implies accurate predictions. We later present nonconformity scores to obtain prediction regions for uncontrollable agents over multiple time steps. Given a failure probability $\delta \in (0, 1)$, our goal is to compute C

from $R^{(1)}, \dots, R^{(K)}$ such that the probability of $R^{(0)}$ being bounded by C is not smaller than $1 - \delta$, i.e., such that

$$\text{Prob}(R^{(0)} \leq C) \geq 1 - \delta.$$

By the results in Lemma 1 of [59], we can compute

$$C := \text{Quantile}_{1-\delta}(R^{(1)}, \dots, R^{(K)}, \infty)$$

as the $(1 - \delta)$ th quantile over the empirical distribution of $R^{(1)}, \dots, R^{(K)}$ and ∞ .¹ By assuming that $R^{(1)}, \dots, R^{(K)}$ are sorted in non-decreasing order and by adding $R^{(K+1)} := \infty$, we have that $C = R^{(p)}$ where $p := \lceil (K + 1)(1 - \delta) \rceil$, i.e., C is the p th smallest nonconformity score. To obtain meaningful prediction regions, we remark that $K \geq \lceil (K + 1)(1 - \delta) \rceil$ has to hold. Otherwise we get $C = \infty$. Lastly, note that the guarantees $\text{Prob}(R^{(0)} \leq C) \geq 1 - \delta$ are marginal over the randomness in $R^{(0)}, R^{(1)}, \dots, R^{(K)}$ (with C depending on $R^{(1)}, \dots, R^{(K)}$) as opposed to being conditional on $R^{(1)}, \dots, R^{(K)}$.

In the following, the open-loop controller is introduced in Sections 3 and 4, and we propose the closed-loop controller in Section 5.

3 Open-Loop Prediction Regions for Multiple Uncontrollable Agents

To solve Problem 1, we use trajectory predictions and compute probabilistic prediction regions for each uncontrollable agent that are valid over multiple time steps. Recall that $Y_{\tau,i}$ denotes the random state of agent i at time τ , and let $\hat{Y}_{\tau|0,i}$ denote the prediction of $Y_{\tau,i}$ made at time $k = 0$.

We are interested in constructing prediction regions for all predictions $\tau \in \{1, \dots, T_\phi\}$ made at time $k := 0$ and for all agents $i \in \{1, \dots, N\}$, i.e., such that

$$\text{Prob}(\|Y_{\tau,i} - \hat{Y}_{\tau|0,i}\| \leq C_{\tau|0,i}, \forall (\tau, i) \in \{1, \dots, T_\phi\} \times \{1, \dots, N\}) \geq 1 - \delta, \quad (3)$$

where $C_{\tau|0,i}$ indicates the τ -step ahead prediction error of agent i for predictions $\hat{Y}_{\tau|0,i}$.

Data-efficient and accurate prediction regions. Computing τ -step ahead prediction regions via $C_{\tau|0,i}$ is in general difficult. Existing works [16, 60] are conservative, data-inefficient, and do not provide prediction regions for multiple agents. The reason is that $C_{\tau|0,i}$ are independently computed for all $(\tau, i) \in \{1, \dots, T_\phi\} \times \{1, \dots, N\}$. This independent computation is followed by a conservative and inefficient union bounding argument (more details below).

Instead, we obtain these prediction regions jointly by extending the framework in [61] to incorporate multiple agents. For the open-loop case, we define the normalized nonconformity score

$$R_{OL}^{(j)} := \max_{\substack{(\tau, i) \in \{1, \dots, T_\phi\} \\ \times \{1, \dots, N\}}} \frac{\|Y_{\tau,i}^{(j)} - \hat{Y}_{\tau|0,i}^{(j)}\|}{\sigma_{\tau|0,i}} \quad (4)$$

for calibration trajectories $Y^{(j)} \in D_{cal}$ where $\sigma_{\tau|0,i} > 0$ are constants that normalize the prediction error to $[0, 1]$ for all times τ and agents i . This nonconformity score is inspired by [62], where a mixed integer linear complementarity program is used to find optimal constants $\sigma_{\tau|0,i}$. However, we do not need to solve nonconvex optimization problems and instead simply normalize over the training dataset D_{train} which has practical advantages. Specifically, we use the normalization

¹Formally, we define the quantile function as $\text{Quantile}_{1-\delta}(R^{(1)}, \dots, R^{(K)}, \infty) := \inf\{z \in \mathbb{R} \mid \text{Prob}(Z \leq z) \geq 1 - \delta\}$ with the random variable $Z := 1/(K + 1)(\sum_i \delta_{R^{(i)}} + \delta_\infty)$ where $\delta_{R^{(i)}}$ and δ_∞ are dirac distributions centered at $R^{(i)}$ and ∞ , respectively.

$\sigma_{\tau|0,i} := \max_j \|Y_{\tau,i}^{(j)} - \hat{Y}_{\tau|0,i}^{(j)}\|$ for training trajectories $Y^{(j)} \in D_{train}$ with the assumption that $\sigma_{\tau|0,i}$ is non-zero. This is important as the optimization problem in [62] may have no solution, or the optimal solution cannot be found due to the nonconvexity of the problem, or it takes too long to solve in practice, especially for large T_ϕ and N . The reader can find an empirical comparison in Section 6.1, where we show that we can obtain similar prediction regions as [62], but in a computationally more efficient manner.

The intuitions behind the nonconformity score in (4) are that normalization via $\sigma_{\tau|0,i}$ will prevent the prediction error $\|Y_{\tau,i}^{(j)} - \hat{Y}_{\tau|0,i}^{(j)}\|$ for a specific agent and time to dominate the max operator. This would result in overly conservative prediction regions for other times and agents.

Valid Prediction Regions with Conformal Prediction. We can now apply conformal prediction, as introduced in Section 2.2, to the open-loop nonconformity score $R_{OL}^{(j)}$. By re-normalizing these nonconformity scores, we then obtain prediction regions as in equations (3).

Theorem 1 *Given the random trajectory $Y := (Y_0, Y_1, \dots) \sim \mathcal{D}$, a set of trajectories D_{cal} and D_{train} that satisfy Assumption 1, and the failure probability $\delta \in (0, 1)$, then the prediction regions in equation (3) hold for the choice of*

$$C_{\tau|0,i} := C_{OL}\sigma_{\tau|0,i}, \quad (5)$$

where $\sigma_{\tau|0,i}$ are positive constants and

$$C_{OL} := \text{Quantile}_{1-\delta}(R_{OL}^{(1)}, \dots, R_{OL}^{(K)}, \infty).$$

Proof. For a test trajectory $Y := (Y_0, Y_1, \dots) \sim \mathcal{D}$, we immediately know from conformal prediction that

$$\text{Prob}\left(\max_{\substack{(\tau,i) \in \{1, \dots, T_\phi\} \\ \times \{1, \dots, N\}}} \frac{\|Y_{\tau,i} - \hat{Y}_{\tau|0,i}\|}{\sigma_{\tau|0,i}} \leq C_{OL}\right) \geq 1 - \delta \quad (6)$$

by construction of C_{OL} . We then see that equation (6) implies that

$$\text{Prob}\left(\frac{\|Y_{\tau,i} - \hat{Y}_{\tau|0,i}\|}{\sigma_{\tau|0,i}} \leq C_{OL}, \forall (\tau, i) \in \{1, \dots, T_\phi\} \times \{1, \dots, N\}\right) \geq 1 - \delta. \quad (7)$$

Since $\sigma_{\tau|0,i} > 0$, we can multiply the inequality in (7) with $\sigma_{\tau|0,i}$. We then see that (3) is valid with the choice of $C_{\tau|0,i} := C_{OL}\sigma_{\tau|0,i}$ which completes the proof. \square

Comparison with existing work. With slight modification of [16, 60], an alternative approach for obtaining $C_{\tau|0,i}$ would be to compute $C_{\tau|0,i} := \text{Quantile}_{1-\delta/(T_\phi N)}(R^{(1)}, \dots, R^{(K)}, \infty)$ with the nonconformity score $R^{(j)} := \|Y_{\tau,i} - \hat{Y}_{\tau|0,i}\|$. However, it is evident that taking the $1 - \delta$ quantile in Theorem 1 compared to the $1 - \delta/(T_\phi N)$ quantile is much more data inefficient. Specifically, for a fixed $\delta \in (0, 1)$, we only require $K \geq (1 - \delta)/\delta$ calibration trajectories as opposed to $K \geq (T_\phi N - \delta)/\delta$ calibration trajectories.² Intuitively, it is also evident that our choice of normalization constants $\sigma_{\tau|0,i}$ provides less conservative prediction regions in practice as evaluating the $1 - \delta$ quantile is more favorable compared to the $1 - \delta/(T_\phi N)$ for larger task horizons T_ϕ and number of agents N . Finally, we remark that one could even consider obtaining conditional guarantees using conditional conformal prediction [63]. Similarly, we can use versions of robust

²Computing the $1 - \delta$ and $1 - \delta/(T_\phi N)$ quantiles requires that $\lceil (K+1)(1-\delta) \rceil \leq K$ and $\lceil (K+1)(1-\delta/(T_\phi N)) \rceil \leq K$, respectively.

conformal prediction to be robust against distribution shifts [51, 59, 61], e.g., caused by interaction between the system in (1) and the distribution \mathcal{D} .

For practitioners. We summarize our method to obtain the prediction regions in equation (3) via Theorem 1 in Algorithm 1, which is executed offline. We note that, in order to compute C_{OL} , we sort the corresponding nonconformity scores (after adding $R_{OL}^{(K+1)} := \infty$) in nondecreasing order and set C_{OL} to be the p th smallest nonconformity score where $p := \lceil (K+1)(1-\delta) \rceil$, as explained in Section 2.2. Specifically, the variable p is set in line 1. We then compute the predictions $\hat{Y}_{\tau|0,i}^{(j)}$ for all calibration data in lines 2-5 and calculate the normalization constants $\sigma_{\tau|0,i}$ over the training data in line 6. Finally, we compute the nonconformity scores $R_{OL}^{(j)}$ for all calibration data in lines 7-9 and apply conformal prediction to obtain C_{OL} in lines 10-11. According to Theorem 1, we then obtain the open-loop prediction regions $C_{\tau|0,i}$.

Algorithm 1: Multi-Agent Prediction Regions (Offline)

Input: failure probability δ , dataset D , horizon T_ϕ

Output: Constants C_{OL} and $\sigma_{\tau|0,i}$

```

1  $p \leftarrow \lceil (K+1)(1-\delta) \rceil$ 
2 forall  $i \in \{1, \dots, N\}$  do
3   forall  $\tau \in [k+1, T_\phi]$  do
4     forall  $j \in \{1, \dots, \bar{K}\}$  do
5        $\left[ \text{Compute } \hat{Y}_{\tau|0,i}^{(j)} \text{ from } (Y_{0,i}^{(j)}, \dots, Y_{k,i}^{(j)}) \right.$ 
6        $\left. \sigma_{\tau|0,i} \leftarrow \max_{j \in \{K+1, \dots, \bar{K}\}} \|Y_{\tau,i}^{(j)} - \hat{Y}_{\tau|0,i}^{(j)}\| \right]$ 
7 forall  $j \in \{1, \dots, K\}$  do
8    $\left[ \text{Compute } R_{OL}^{(j)} \text{ as in equation (4)} \right.$ 
9    $\left. \text{Set } R_{OL}^{(K+1)} \leftarrow \infty \right]$ 
10 Sort  $R_{OL}^{(j)}$  in nondecreasing order
11 Set  $C_{OL} \leftarrow R_{OL}^{(p)}$ 

```

4 Open-Loop Predictive STL Control Synthesis

In this section, we use the previously computed prediction regions and design predictive controllers that solve Problem 1, i.e., controllers u that ensure that x is such that $\text{Prob}(\mathbf{S} \models \phi) \geq 1 - \delta$. Specifically, we use the prediction regions and present an MIP encoding for the STL task ϕ . We first present a qualitative and a quantitative encoding using the Boolean and quantitative semantics of ϕ in Sections 4.1 and 4.2, respectively. In Section 4.3, we then use these encodings and present the open-loop controller.

4.1 Qualitative STL Encoding with Multi-Agent Prediction Regions

A standard way of encoding STL tasks for deterministic trajectories \mathbf{s} is by using an MIP encoding [27, 46]. The idea is to introduce a binary variable z_0^ϕ and a set of mixed integer constraints over \mathbf{s} such that $z_0^\phi = 1$ if and only if $\mathbf{s} \models \phi$. In this paper, however, we deal with stochastic trajectories \mathbf{S} that consist of the system trajectory x and the stochastic trajectories of dynamic agents Y . We will instead introduce a binary variable \bar{z}_0^ϕ and a set of mixed integer constraints over x and the

prediction regions in (3) such that $\bar{z}_0^\phi = 1$ implies that $\mathbf{S} \models \phi$ with a probability of at least $1 - \delta$. In this way, \bar{z}_0^ϕ can be seen as a probabilistic version of z_0^ϕ . We emphasize that our MIP encoding provides sufficient but not necessary conditions for the task satisfaction. Specifically, we can not guarantee necessity due to the use of probabilistic prediction regions.

In the remainder, we generate the mixed integer constraints that define \bar{z}_0^ϕ recursively on the structure of ϕ . Our main innovation is a probabilistic MIP encoding for predicates, while the encoding of Boolean and temporal operators follows [27, 46]. We here recall from Assumption 2 that the formula ϕ is in positive normal form so that we do not need to consider negations. To provide a general encoding that can be used for open-loop and closed-loop control, we let $k \geq 0$ denote the current time. For the open-loop case, we only need to consider the initial time, i.e., $k = 0$. As we will treat the system state x_k separately from the state of uncontrollable dynamic agents Y_k contained in S_k , we will write $\mu(x_k, Y_k)$ instead of $\mu(s_k)$.

Predicates π^μ . Let us denote the set of predicates π^μ in ϕ by \mathcal{P} . Now, for each predicate $\pi^\mu \in \mathcal{P}$ and for each time $\tau \geq 0$, we introduce a binary variable $\bar{z}_{\tau|k}^\mu \in \{0, 1\}$. If $\tau \leq k$, then we have observed the value of Y_τ already, and we set $\bar{z}_{\tau|k}^\mu = 1$ if and only if $\mu(x_\tau, Y_\tau) \geq 0$. If $\tau > k$, then we would like to constrain $\bar{z}_{\tau|k}^\mu$ such that $\bar{z}_{\tau|k}^\mu = 1$ implies $\text{Prob}(\mu(x_{\tau|k}, Y_\tau) \geq 0) \geq 1 - \delta$. Motivated by Theorem 1, we use the Big-M method and define the constraint

$$- \min_{y \in \mathcal{B}_{\tau|k}} \mu(x_{\tau|k}, y) \leq M(1 - \bar{z}_{\tau|k}^\mu) - \epsilon, \quad (8)$$

where M and ϵ are sufficiently large and sufficiently small positive constants, respectively, see [27, 64] for more details. The minimization of $\mu(x_{\tau|k}, y)$ over the y component within the set $\mathcal{B}_{\tau|k}$ will account for all Y_τ that are contained within our probabilistic prediction regions. Specifically, the set $\mathcal{B}_{\tau|k}$ contains all states contained within a geometric norm ball that is centered around the predictions $\hat{Y}_{\tau|k,i}$ with a size of $C_{\tau|k,i}$ and is defined as

$$\mathcal{B}_{\tau|k} := \{[y_1, \dots, y_N]^\top \in \mathbb{R}^{n_y} \mid \forall i \in \{1, \dots, N\}, \|y_i - \hat{Y}_{\tau|k,i}\| \leq C_{\tau|k,i}\}. \quad (9)$$

In the case when $k = 0$, we use the values of $C_{\tau|0,i}$ as in (5) that define the open-loop prediction region in (3). This implies that $\text{Prob}(Y_\tau \in \mathcal{B}_\tau, \tau \in \{1, \dots, T_\phi\}) \geq 1 - \delta$.

By Theorem 1 and the construction in equation (8), we have the following straightforward result.

Corollary 1 *If $\bar{z}_{\tau|0}^\mu = 1$ for all pairs $(\tau, \pi^\mu) \in TP$, where $TP \subseteq \{0, \dots, T_\phi\} \times \mathcal{P}$ is the set of some pairs, then it holds that $\text{Prob}(\mu(x_{\tau|0}, Y_\tau) \geq 0, \forall (\tau, \pi^\mu) \in TP) \geq 1 - \delta$.*

Proof. If $\bar{z}_{\tau|0}^\mu = 1$ for all pairs $(\tau, \pi^\mu) \in TP$, then it follows by equation (8) that $x_{\tau|0}$ is such that $0 < \epsilon \leq \min_{y \in \mathcal{B}_{\tau|0}} \mu(x_{\tau|0}, y)$ for all pairs $(\tau, \pi^\mu) \in TP$. Now, using Theorem 1 (Equation (3)), we can directly conclude that $\text{Prob}(\mu(x_{\tau|0}, Y_\tau) \geq 0, \forall (\tau, \pi^\mu) \in TP) \geq 1 - \delta$. \square

Remark 1 *We do not need to enforce $\bar{z}_{\tau|k}^\mu = 0$ since the STL formula ϕ is in positive normal form as per Assumption 2. However, by using the constraint $\max_{y \in \mathcal{B}_{\tau|k}} \mu(x_{\tau|k}, y) \leq M\bar{z}_{\tau|k}^\mu - \epsilon$ we could enforce that $\bar{z}_{\tau|k}^\mu = 0$ implies $\text{Prob}(\mu(x_{\tau|k}, Y_\tau) < 0, \forall (\tau, \pi^\mu) \in TP) \geq 1 - \delta$.*

Computational considerations. Note that we minimize $\mu(x_{\tau|k}, y)$ over the y component within the ball $\mathcal{B}_{\tau|k}$ in equation (8). In an outer loop, we will additionally need to optimize over $x_{\tau|k}$ to compute control inputs $u_{\tau|k}$. To obtain computational tractability for this, we will now

remove the minimum over y and instead write equation (8) in closed-form. Since the function μ is continuously differentiable and convex in its parameters by Assumption 2, we can use the KKT conditions of the inner problem to do so. Specifically, the constraints in equation (8) can be converted into a bilevel optimization problem where the outer problem consists of the constraints

$$-\mu(x_{\tau|k}, y^*) \leq M(1 - \bar{z}_{\tau|k}^\mu) - \epsilon, \quad (10)$$

and where the inner optimization problem is

$$y^* := \underset{y}{\operatorname{argmin}} \mu(x_{\tau|k}, y), \quad (11a)$$

$$\text{s.t. } \|y_i - \hat{Y}_{\tau|k,i}\| \leq C_{\tau|k,i}, \forall i \in \{1, \dots, N\}. \quad (11b)$$

We can use the KKT conditions of the inner optimization problem in (11) after a minor modification in which we change the constraints $\|y_i - \hat{Y}_{\tau|k,i}\| \leq C_{\tau|k,i}$ into $(y_i - \hat{Y}_{\tau|k,i})^\top (y_i - \hat{Y}_{\tau|k,i}) \leq C_{\tau|k,i}^2$ to obtain differentiable constraint functions. Formally, we obtain

$$\frac{\partial \mu(x_{\tau|k}, y^*)}{\partial y} + \sum_{i=1}^N \lambda_i \frac{\partial (y_i^* - \hat{Y}_{\tau|k,i})^\top (y_i^* - \hat{Y}_{\tau|k,i})}{\partial y_i} = 0 \quad (12a)$$

$$(y_i^* - \hat{Y}_{\tau|k,i})^\top (y_i^* - \hat{Y}_{\tau|k,i}) \leq C_{\tau|k,i}^2, \forall i \in \{1, \dots, N\} \quad (12b)$$

$$\lambda_i \geq 0, \forall i \in \{1, \dots, N\} \quad (12c)$$

$$\lambda_i ((y_i^* - \hat{Y}_{\tau|k,i})^\top (y_i^* - \hat{Y}_{\tau|k,i}) - C_{\tau|k,i}^2) = 0, \forall i \in \{1, \dots, N\} \quad (12d)$$

as the set of KKT conditions for the inner problem in (11).

We have that a solutions y^* to (11) is a feasible solution to the KKT conditions in (12) and vice versa [65], since Slater's condition holds for the inner convex optimization problem (11), with the reasoning that $C_{\tau|k,i} > 0$ due to $\sigma_{\tau|0,i} > 0$ ³. As a result, we can replace (8) with equations (10) and (12) equivalently.

Boolean and temporal operators. So far, we have encoded predicates π^μ . We can encode Boolean and temporal operators recursively using the standard MIP encoding [27, 46]. In brief, for the conjunction $\phi := \bigwedge_{i=1}^m \phi_i$ we introduce the binary variable $\bar{z}_{\tau|k}^\phi \in \{0, 1\}$ that is such that $\bar{z}_{\tau|k}^\phi = 1$ if and only if $\bar{z}_{\tau|k}^{\phi_1} = \dots = \bar{z}_{\tau|k}^{\phi_m} = 1$. Consequently, $\bar{z}_{\tau|k}^\phi = 1$ implies that $(\mathbf{S}, \tau) \models \phi$ holds with a probability of at least $1 - \delta$ at time step k . We achieve this by enforcing the constraints

$$\begin{aligned} \bar{z}_{\tau|k}^\phi &\leq \bar{z}_{\tau|k}^{\phi_i}, i = 1, \dots, m, \\ \bar{z}_{\tau|k}^\phi &\geq 1 - m + \sum_{i=1}^m \bar{z}_{\tau|k}^{\phi_i}. \end{aligned}$$

For the disjunction $\phi := \bigvee_{i=1}^m \phi_i$, we follow the same idea but instead enforce the constraints

$$\begin{aligned} \bar{z}_{\tau|k}^\phi &\geq \bar{z}_{\tau|k}^{\phi_i}, i = 1, \dots, m, \\ \bar{z}_{\tau|k}^\phi &\leq \sum_{i=1}^m \bar{z}_{\tau|k}^{\phi_i}. \end{aligned}$$

For temporal operators, we follow a similar procedure, but first note that temporal operators can be written as Boolean combinations of conjunctions and disjunctions. For $\phi := \mathbf{G}_{[a,b]} \phi_1$, we again introduce a binary variable $\bar{z}_{\tau|k}^\phi \in \{0, 1\}$ and encode $\bar{z}_{\tau|k}^\phi = \bigwedge_{\tau'=\tau+a}^{\tau+b} \bar{z}_{\tau'|k}^{\phi_1}$ using the MIP constraints

³Here, we make a mild assumption that $C_{OL} \neq 0$.

for conjunctions introduced before. Similarly, for $\phi := \mathbf{F}_{[a,b]}\phi_1$ we use that $\bar{z}_{\tau|k}^\phi = \bigvee_{\tau'=\tau+a}^{\tau+b} \bar{z}_{\tau'|k}^{\phi_1}$, while for $\phi = \phi_1 \mathbf{U}_{[a,b]}\phi_2$ we use that $\bar{z}_{\tau|k}^\phi = \bigvee_{\tau'=\tau+a}^{\tau+b} (\bar{z}_{\tau'|k}^{\phi_2} \wedge \bigwedge_{\tau''=\tau}^{\tau'} \bar{z}_{\tau''|k}^{\phi_1})$.

Soundness of the encoding. At the initial time step $k = 0$, the procedure described above provides us with a binary variable $\bar{z}_{0|0}^\phi$ and a set of mixed integer constraints over x such that $\bar{z}_{0|0}^\phi = 1$ implies that $\mathbf{S} \models \phi$ holds with a probability of at least $1 - \delta$. We summarize this result next, and we introduce the result of closed-loop in the next section.

Theorem 2 (Open-loop qualitative encoding result) *Let the conditions from Problem 1 hold. If $\bar{z}_{0|0}^\phi = 1$, then we have that $\text{Prob}(\mathbf{S} \models \phi) \geq 1 - \delta$.*

Proof. By enforcing that $\bar{z}_{0|0}^\phi = 1$, there is an assignment of 0 and 1 values to the binary variables $\bar{z}_{\tau|0}^\mu$ for each pair $(\tau, \pi^\mu) \in \{1, \dots, T_\phi\} \times \mathcal{P}$. This assignment is non-unique. Specifically, let $\bar{z}_{\tau|0}^\mu = 1$ for all pairs $(\tau, \pi^\mu) \in TP$, where $TP \subseteq \{1, \dots, T_\phi\} \times \mathcal{P}$ is the set of some pairs, and let $\bar{z}_{\tau|0}^\mu = 0$ otherwise. By Corollary 1, it follows that $\text{Prob}(\mu(x_{\tau|0}, Y_\tau) \geq 0, \forall (\tau, \pi^\mu) \in TP) \geq 1 - \delta$. By the recursive definition of $\bar{z}_{0|0}^\phi$ using the encoding from [27, 46] for Boolean and temporal operators and since ϕ is in positive normal form, it follows that $\text{Prob}(\mathbf{S} \models \phi) \geq 1 - \delta$. \square

4.2 Quantitative STL Encoding with Multi-Agent Prediction Regions

The qualitative MIP encoding ensures that $\bar{z}_{0|0}^\phi = 1$ implies that $\text{Prob}(\mathbf{S} \models \phi) \geq 1 - \delta$ as in Theorem 2. However, in some cases one may want to optimize over the quantitative semantics $\rho^\phi(\mathbf{S}, 0)$. We next present a quantitative MIP encoding for ϕ . Specifically, we will recursively define a continuous variable $\bar{r}_{0|k}^\phi \in \mathbb{R}$ that will be such that $\rho^\phi(\mathbf{S}, 0) \geq \bar{r}_{0|k}^\phi$ with a probability of at least $1 - \delta$. Our main innovation is a quantitative MIP encoding for predicates, while the Boolean and temporal operators again follow the standard MIP encoding [27, 46].

Predicates. For each predicate $\pi^\mu \in \mathcal{P}$ and for each time $\tau \geq 0$, we introduce a continuous variable $\bar{r}_{\tau|k}^\mu \in \mathbb{R}$. Inspired by [66], we define $\bar{r}_{\tau|k}^\mu$ as

$$\bar{r}_{\tau|k}^\mu := \begin{cases} \mu(x_\tau, Y_\tau) & \text{if } \tau \leq k, \\ \min_{y \in \mathcal{B}_{\tau|k}} \mu(x_{\tau|k}, y) & \text{otherwise} \end{cases} \quad (13)$$

where we again notice that Y_τ is known if $\tau \leq k$, while we compute $\min_{y \in \mathcal{B}_{\tau|k}} \mu(x_{\tau|k}, y)$ if $\tau > k$ to consider the worst case of $\mu(x_{\tau|k}, y)$ for y within the prediction region $\mathcal{B}_{\tau|k}$.

By Theorem 1, which ensures that $Y_\tau \in \mathcal{B}_{\tau|k}$ holds with a probability of at least $1 - \delta$, and the construction in equation (13), we have the following straightforward result.

Corollary 2 *It holds that $\text{Prob}(\rho^\mu(\mathbf{S}, \tau) \geq \bar{r}_{\tau|0}^\mu, \forall (\tau, \pi^\mu) \in \{0, \dots, T_\phi\} \times \mathcal{P}) \geq 1 - \delta$, where $\mathbf{S}_\tau = [x_{\tau|0}, Y_\tau]$.*

Proof. The result follows directly from Theorem 1 (Equation (3)) and the construction of $\bar{r}_{\tau|0}^\mu$ in equation (13) using the prediction region $\mathcal{B}_{\tau|0}$. \square

Similarly to the qualitative encoding, the term $\min_{y \in \mathcal{B}_{\tau|k}} \mu(x_{\tau|k}, y)$ in equation (13) can be written as in equation (11), and we can use equations (12) instead of (11).

Boolean and temporal operators. As for the qualitative encoding, we only provide a brief summary for the quantitative encoding of Boolean and temporal operators that follow standard encoding rules. For the conjunction $\phi := \bigwedge_{i=1}^m \phi_i$, we introduce the continuous variable $\bar{r}_{\tau|k}^\phi \in \mathbb{R}$

that will be such that $\bar{r}_{\tau|k}^\phi = \min\{\bar{r}_{\tau|k}^{\phi_1}, \dots, \bar{r}_{\tau|k}^{\phi_m}\}$. Particularly, we achieve this by enforcing the constraints

$$\begin{aligned} \sum_{i=1}^m p_{\tau|k}^{\phi_i} &= 1, \\ \bar{r}_{\tau|k}^\phi &\leq \bar{r}_{\tau|k}^{\phi_i}, i = 1, \dots, m, \\ \bar{r}_{\tau|k}^{\phi_i} - (1 - p_{\tau|k}^{\phi_i})M &\leq \bar{r}_{\tau|k}^\phi \leq \bar{r}_{\tau|k}^{\phi_i} + M(1 - p_{\tau|k}^{\phi_i}), i = 1, \dots, m, \end{aligned}$$

where $p_{\tau|k}^{\phi_i} \in \{0, 1\}$ are m new binary variables so that $\bar{r}_{\tau|k}^\phi = r_{\tau|k}^{\phi_i}$ if and only if $p_{\tau|k}^{\phi_i} = 1$. By this encoding, $\bar{r}_{\tau|k}^\phi \geq 0$ implies that $(\mathbf{S}, \tau) \models \phi$ holds with a probability of at least $1 - \delta$. For the disjunction $\phi := \bigvee_{i=1}^m \phi_i$, we follow the same idea but instead enforce the constraints

$$\begin{aligned} \sum_{i=1}^m p_{\tau|k}^{\phi_i} &= 1, \\ \bar{r}_{\tau|k}^\phi &\geq \bar{r}_{\tau|k}^{\phi_i}, i = 1, \dots, m, \\ \bar{r}_{\tau|k}^{\phi_i} - (1 - p_{\tau|k}^{\phi_i})M &\leq \bar{r}_{\tau|k}^\phi \leq \bar{r}_{\tau|k}^{\phi_i} + M(1 - p_{\tau|k}^{\phi_i}), i = 1, \dots, m. \end{aligned}$$

For temporal operators, we again note that we can write each operator as Boolean combinations of conjunctions and disjunctions and then follow the same procedure as for the qualitative encoding.

Soundness of the encoding. At the initial time step $k = 0$, the procedure described above gives us a continuous variable $\bar{r}_{0|0}^\phi$ and a set of mixed integer constraints over x such that $\bar{r}_{0|0}^\phi$ is a probabilistic lower bound of $\rho^\phi(\mathbf{S}, 0)$. We summarize this result next, and provide the closed-loop result in the next section.

Theorem 3 (Open-loop quantitative encoding result) *Let the conditions from Problem 1 hold. It holds that $\text{Prob}(\rho^\phi(\mathbf{S}, 0) \geq \bar{r}_{0|0}^\phi) \geq 1 - \delta$. If $\bar{r}_{0|0}^\phi > 0$, then we have that $\text{Prob}(\mathbf{S} \models \phi) \geq 1 - \delta$.*

Proof. Recall that $\text{Prob}(\rho^\mu(\mathbf{S}, \tau) \geq \bar{r}_{\tau|0}^\mu, \forall (\tau, \pi^\mu) \in \{0, \dots, T_\phi\} \times \mathcal{P}) \geq 1 - \delta$ by Corollary 2. Since the task ϕ is in positive normal form, which excludes negations, and due to the recursive structure of ϕ we can directly conclude that $\text{Prob}(\rho^\phi(\mathbf{S}, 0) \geq \bar{r}_{0|0}^\phi) \geq 1 - \delta$. If $\bar{r}_{0|0}^\phi > 0$, we can obviously conclude that $\text{Prob}(\mathbf{S} \models \phi) \geq 1 - \delta$. \square

We emphasize that the previous result will allow us to directly optimize over the variable $\bar{r}_{0|0}^\phi$ to achieve $\bar{r}_{0|0}^\phi > 0$, which then implies that $\text{Prob}(\mathbf{S} \models \phi) \geq 1 - \delta$.

We note that the quantitative encoding allows for robustness considerations and provides a more fine-grained analysis. The qualitative encoding, on the other hand, is computationally more tractable.

4.3 Predictive MIP-Based Control Synthesis

For control synthesis, we can now use the qualitative encoding via the binary variable $\bar{z}_{0|k}^\phi$ or the quantitative encoding via the continuous variable $\bar{r}_{0|k}^\phi$ to solve Problem 1. Formally, we then solve the following qualitative mixed integer optimization problem

$$\mathbf{u}_{k:T_\phi-1}^* := \underset{\mathbf{u}_{k:T_\phi-1}}{\text{argmin}} J(x_k, \mathbf{u}_{k:T_\phi-1}) \quad (14a)$$

subject to

$$\mathbf{u}_{k:T_\phi-1} \in \mathcal{U}^{T_\phi-k}, \mathbf{x}_{k+1:T_\phi} \in \mathcal{X}^{T_\phi-k} \quad (14b)$$

$$x_{\tau+1} = f(x_\tau, u_\tau), \tau = k, \dots, T_\phi - 1, \quad (14c)$$

$$\bar{z}_{0|k}^\phi = 1. \quad (14d)$$

Similarly, the quantitative mixed integer optimization problem can be formulated by replacing $\bar{z}_{0|k}^\phi = 1$ with $\bar{r}_{0|k}^\phi > 0$ in equation (14d).

Note particularly that we enforce either $\bar{z}_{0|k}^\phi = 1$ or $\bar{r}_{0|k}^\phi > 0$ in equation (14d). This enables us to select between the quantitative and the qualitative encoding. We can also enforce $\bar{r}_{0|k}^\phi > a$, where $a > 0$, to obtain a trajectory with higher robustness.

Open-loop synthesis. We will start with analyzing the case when $k = 0$ where we get an open-loop control sequence $\mathbf{u}_{0:T_\phi-1}^*$. By Theorems 2 and 3 it is easy to see that we solve Problem 1 if we can find a feasible solution to the optimization problem in (14). We next summarize the result that solves Problem 1.

Theorem 4 (Open-loop control) *Let the conditions from Problem 1 hold. If the optimization problem in (14) is feasible at time $k = 0$, then applying the open-loop control sequence $\mathbf{u}_{0:T_\phi-1}^*$ to (1) results in*

$$\text{Prob}(\mathbf{S} \models \phi) \geq 1 - \delta.$$

Proof. Note that we enforce that either $\bar{z}_{0|0}^\phi = 1$ or $\bar{r}_{0|0}^\phi > 0$ within the optimization problem in (14). By Theorems 2 and 3 this implies that $\text{Prob}(\mathbf{S} \models \phi) \geq 1 - \delta$ or $\text{Prob}(\rho^\phi(\mathbf{S}, 0) \geq \bar{r}_{0|0}^\phi) \geq 1 - \delta$, respectively. \square

The complexity of the optimization problem in (14) is in general that of a mixed integer program which is NP-hard.

5 Closed-Loop Predictive STL Control Synthesis

The above open-loop control strategy may be conservative as the prediction regions $C_{\tau|0,i}$ will usually be conservative for large τ as then the predictions $\hat{Y}_{\tau|0}$ lose accuracy. Furthermore, due to the lack of state feedback, the open-loop controller is not robust. Therefore, we propose to solve the optimization problem in (14) in a receding horizon fashion as in [16].

An intuitive solution to this problem is the MPC framework as follows. At each time k we observe the realization of Y_k , update our predictions $\hat{Y}_{\tau|k}$, and compute the control sequence $\mathbf{u}_{k:T_\phi-1}^*$ by solving the optimization problem in (14). Then, we apply the first element u_k^* of $\mathbf{u}_{k:T_\phi-1}^*$ to the system in (1) before we repeat the process. However, since the STL task is defined over the whole trajectory \mathbf{S} (instead of state constraints $c(x_k, Y_k) \geq 0$ in [16]), we cannot apply this strategy and get the same result as in [16]. This poses a new challenge that we address here. Specifically, [16] show that $\text{Prob}(c(x_k, Y_k) \geq 0, \forall k \in \{1, \dots, T\}) \geq 1 - \delta$, where T is the length of the task, if the underlying optimization problem is feasible at all time steps. However, this reasoning cannot be applied to the STL case for the following reason. Our optimization problem (14) depends on both past realizations and future predictions, as opposed to [16], where the optimization problem only depends on future predictions, but not past realizations. Indeed, past realizations affect the satisfaction of the STL specification and can hence break the feasibility of the optimization problem. The authors in [67] build upon [16] and present a recursively feasible shrinking horizon MPC that guarantees probabilistic satisfaction of state constraints. However, this strategy cannot be applied to the STL case for the same reasons since feasibility is affected by past realizations.

We propose a closed-loop control framework for STL tasks that is recursively feasibility with high probability. We use the qualitative and quantitative encodings presented in Sections 4.1 and 4.2, respectively, and the optimization problem (14) presented in Section 4.3 where we modify the constraints imposed for predicates, while we keep the constraints for Boolean and temporal operators without modification. In order to change the constraints for predicates, we need new prediction regions which we present in Section 5.1 before we discuss the qualitative and quantitative encodings in Section 5.2 as well as the closed-loop controller in Section 5.3.

5.1 Closed-Loop Prediction Regions

We now apply conformal prediction to capture the union of past prediction regions, which will allow us to design a shrinking-horizon MPC with probabilistic recursive feasibility guarantees. Specifically, we are interested in constructing prediction regions for all prediction times $\tau \in \{1, \dots, T_\phi\}$ made at previous times $s \in \{0, \dots, \tau - 1\}$ for all agents $i \in \{1, \dots, N\}$, i.e., such that

$$\text{Prob}(\|Y_{\tau,i} - \hat{Y}_{\tau|s,i}\| \leq C_{\tau|s,i}, \forall (\tau, s, i) \in \{1, \dots, T_\phi\} \times \{0, \dots, \tau - 1\} \times \{1, \dots, N\}) \geq 1 - \delta, \quad (15)$$

where $C_{\tau|s,i}$ indicates the prediction error of agent i for predictions $\hat{Y}_{\tau|s,i}$ made at time s . Intuitively, this guarantees that the probability of Y_τ being in the previous prediction regions described by $C_{\tau|s,i}$ for all previous times $s \in \{0, \dots, \tau - 1\}$ and agents $i \in \{1, \dots, N\}$ is larger than or equal to $1 - \delta$, which will allow us to formulate constraints that guarantee feasibility of the optimization problem (14) (more details follow).

To obtain the prediction region in (15), we follow a similar idea to the open-loop case, but instead define the normalized nonconformity score

$$R_{CL}^{(j)} := \max_{\substack{(\tau, s, i) \in \{1, \dots, T_\phi\} \\ \times \{0, \dots, \tau - 1\} \times \{1, \dots, N\}}} \frac{\|Y_{\tau,i} - \hat{Y}_{\tau|s,i}\|}{\sigma_{\tau|s,i}} \quad (16)$$

for calibration trajectories $Y^{(j)} \in D_{cal}$ where $\sigma_{\tau|s,i} > 0$ are again constants that normalize the prediction error to $[0, 1]$ for all prediction times τ , past times s and agents i . In this case, we let $\sigma_{\tau|s,i} := \max_j \|Y_{\tau,i}^{(j)} - \hat{Y}_{\tau|s,i}^{(j)}\|$ for training trajectories $Y^{(j)} \in D_{train}$, again assuming that $\sigma_{\tau|s,i}$ is non-zero. Then, we have the following theorem.

Theorem 5 *Given the random trajectory $Y := (Y_0, Y_1, \dots) \sim \mathcal{D}$, a set of trajectories D_{cal} and D_{train} that satisfy Assumption 1, and the failure probability $\delta \in (0, 1)$, then the prediction region in equation (15) holds for the choice of*

$$C_{\tau|s,i} := C_{CL} \sigma_{\tau|s,i} \quad (17)$$

where $\sigma_{\tau|s,i}$ is a positive constant and

$$C_{CL} := \text{Quantile}_{1-\delta}(R_{CL}^{(1)}, \dots, R_{CL}^{(K)}, \infty).$$

The proof follows exactly the same steps as Theorem 1 and is omitted. Similarly, we can compute all $C_{\tau|s,i}$ in an offline manner by modifying Algorithm 1.

5.2 Closed-Loop STL Encoding

Future predictions will affect recursive feasibility since the prediction regions made at time $k + 1$ may be different from that made at time k , which makes the optimization problems (14) at time $k + 1$ different from that at time k . To account for this, inspired by [67], we gradually relax the constraints as now prediction regions become available online. Following this idea, we introduce qualitative and quantitative encodings in the remainder.

Qualitative encoding. We replace the quantitative encoding of predicates in equation (8) by

$$-\max_{0 \leq s \leq k} \min_{y \in \mathcal{B}_{\tau|s}} \mu(x_{\tau|k}, y) \leq M(1 - \bar{z}_{\tau|k}^{\mu}) - \epsilon, \quad (18)$$

where $\mathcal{B}_{\tau|s}$ is defined as before in equation (9), but now with $C_{\tau|s,i}$ as in (17). We use s to denote the past time steps, and recall that k is the current time and τ is the prediction time. Equation (18) enforces $-\min_{y \in \mathcal{B}_{\tau|s}} \mu(x_{\tau|k}, y) \leq M(1 - \bar{z}_{\tau|k}^{\mu}) - \epsilon$ to be satisfied for at least one of the prediction regions $\mathcal{B}_{\tau|s}, 0 \leq s \leq k$, instead of the current prediction region $\mathcal{B}_{\tau|k}$. Intuitively, the max operation in (18) allows us to pick the least conservative prediction region to encode the predicate function, which relaxes the constraints gradually. Figure 1 illustrates the aforementioned idea by an example. Specifically, the predicate describes the task of two agents being close with distance of at most two, i.e., $\mu(x, y) = 2 - \|x - y\|$. The two grey areas indicate the feasible areas at different times, i.e., for the constraints $\min_{y \in \mathcal{B}_{2|0}} \mu(x, y) \geq 0$ and $\min_{y \in \mathcal{B}_{2|1}} \mu(x, y) \geq 0$. The maximum operator in equation (18) allows to choose the union of these areas as the feasible set at time step one.

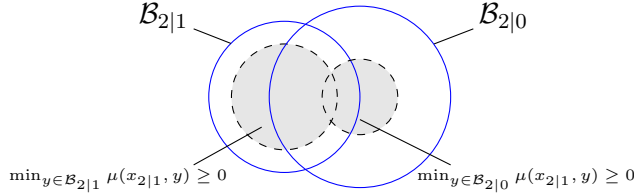


Figure 1: Illustration of the idea of gradual constraint relaxation.

Computational considerations. To obtain computational tractability for (18), we introduce a binary variable for each s as $q_{\tau|k}^{\mu,s}$ to indicate whether the predicate is satisfied under $\mathcal{B}_{\tau|s}$, i.e., $q_{\tau|k}^{\mu,s} = 1$ iff $-\min_{y \in \mathcal{B}_{\tau|s}} \mu(x_{\tau|k}, y) \leq M(1 - \bar{z}_{\tau|k}^{\mu}) - \epsilon$. Specifically, we have the following constraints for each $s, 0 \leq s \leq k$:

$$-\min_{y \in \mathcal{B}_{\tau|s}} \mu(x_{\tau|k}, y) - M(1 - \bar{z}_{\tau|k}^{\mu}) + \epsilon \leq M'(1 - q_{\tau|k}^{\mu,s}) - \epsilon', \quad (19a)$$

$$\min_{y \in \mathcal{B}_{\tau|s}} \mu(x_{\tau|k}, y) + M(1 - \bar{z}_{\tau|k}^{\mu}) - \epsilon \leq M'q_{\tau|k}^{\mu,s} - \epsilon', \quad (19b)$$

where M' and ϵ' are sufficiently large and sufficiently small positive constants similar to M and ϵ . For simplicity, we can choose $M' = M$ and $\epsilon' = \epsilon$. Then, instead of enforcing (18), we enforce (19) together with

$$\sum_{s=0}^k q_{\tau|k}^{\mu,s} \geq 1. \quad (20)$$

By enforcing (20), it holds that $q_{\tau|k}^{\mu,s} = 1$ for at least one $s \in \{0, \dots, k\}$, so that $-\min_{y \in \mathcal{B}_{\tau|s}} \mu(x_{\tau|k}, y) \leq M(1 - \bar{z}_{\tau|k}^{\mu}) - \epsilon$ holds for at least one of $\mathcal{B}_{\tau|s}$, which implies that (18) holds. In the

opposite direction, if $-\min_{y \in \mathcal{B}_{\tau|s}} \mu(x_{\tau|k}, y) \leq M(1 - \bar{z}_{\tau|k}^\mu) - \epsilon$ holds under $\mathcal{B}_{\tau|s}$, then $q_{\tau|k}^{\mu,s} = 1$ and (20) holds. As a result, we can use equations (19) and (20) to replace (18).

Summary of qualitative encoding. To encode $\bar{z}_{0|k}^\phi$ in the optimization problem (14), we encode predicates by equations (19) and (20) instead of equation (8). Additionally, we encode Boolean and temporal operators in the same way as in the open-loop case in Section 4.1.

Quantitative encoding. Similarly, we encode predicates by gradually relaxed constraints for the quantitative encoding. Specifically, we replace the quantitative encoding of predicates in equation (13) by

$$\bar{r}_{\tau|k}^\mu := \begin{cases} \mu(x_\tau, Y_\tau) & \text{if } \tau \leq k, \\ \max_{0 \leq s \leq k} \min_{y \in \mathcal{B}_{\tau|s}} \mu(x_{\tau|k}, y) & \text{otherwise.} \end{cases} \quad (21)$$

Intuitively, instead of considering the worst case of $\mu(x_{\tau|k}, y)$ for y within the prediction region $\mathcal{B}_{\tau|k}$, we choose the least conservative prediction region from $\mathcal{B}_{\tau|s}, 0 \leq s \leq k$ to encode the predicate by the maximum operator.

Computational considerations. To obtain computational tractability for the maximum operator when $\tau > k$ in equation (21), we apply a similar idea as for the Boolean encoding of the disjunction operator by introducing the binary variable $q_{\tau|k}^{\mu,s}$ to indicate which value is the largest. Specifically, we use the following constraints to replace (21) in the case that $\tau > k$:

$$\sum_{s=0}^k q_{\tau|k}^{\mu,s} = 1, \quad (22a)$$

$$\bar{r}_{\tau|k}^\mu \geq \min_{y \in \mathcal{B}_{\tau|s}} \mu(x_{\tau|k}, y), s = 0, \dots, k, \quad (22b)$$

$$\bar{r}_{\tau|k}^\phi \leq \min_{y \in \mathcal{B}_{\tau|s}} \mu(x_{\tau|k}, y) + M(1 - q_{\tau|k}^{\mu,s}), s = 0, \dots, k, \quad (22c)$$

$$\bar{r}_{\tau|k}^\phi \geq \min_{y \in \mathcal{B}_{\tau|s}} \mu(x_{\tau|k}, y) - (1 - q_{\tau|k}^{\mu,s})M, s = 0, \dots, k. \quad (22d)$$

Consequently, $q_{\tau|k}^{\mu,s} = 1$ iff $\bar{r}_{\tau|k}^\mu = \min_{y \in \mathcal{B}_{\tau|s}} \mu(x_{\tau|k}, y)$.

Summary of quantitative encoding. To encode $\bar{r}_{0|k}^\phi$ in the optimization problem (14), we encode predicates by equations (21) and (22) instead of equation (13). We again encode Boolean and temporal operators in the same way as in the closed-loop case in Section 4.2.

5.3 Closed-Loop Predictive MIP-Based Control Synthesis

In this subsection, we present our closed-loop control framework. At each time k , we observe the realization of Y_k , compute the control sequence $\mathbf{u}_{k:T_\phi-1}^* := u_{k|k}^*, \dots, u_{T_\phi-1|k}^*$ based on the previous prediction regions $\mathcal{B}_{\tau|s}, 0 \leq s \leq k$, by solving the optimization problem in (14), where $\bar{z}_{0|k}^\phi$ and $\bar{r}_{0|k}^\phi$ are encoded as we described in the last subsection. Then, we apply the first element u_k^* of $\mathbf{u}_{k:T_\phi-1}^*$ to the system in (1) before we repeat the process. Naturally, we do so in a shrinking horizon manner where the prediction horizon decreases by one at each time.

Theorem 6 (Closed-loop control) *Let the conditions from Problem 1 hold. Suppose the optimization problem in (14) is feasible at the initial time $k = 0$, where the predicates are encoded as in (19) and (20) (qualitative encoding) or (22) (quantitative encoding). Then, the probability of (14) being feasible at every time step $k \in \{1, \dots, T_\phi - 1\}$ is larger than or equal to $1 - \delta$. Furthermore, applying $u_{k|k}^*$ results in $\text{Prob}(\mathbf{S} \models \phi) \geq 1 - \delta$.*

Proof. For brevity, we only show the qualitative case, while the proof for the quantitative case follows exactly the same steps. At time k , assume that we have obtained the optimal solution $\mathbf{u}_{k:T_\phi-1}^* := u_{k|k}^*, \dots, u_{T_\phi-1|k}^*$ for the optimization problem (14) such that $\bar{z}_{0|k}^\phi = 1$. This means that there is an assignment of 0 and 1 values of the binary variables $\bar{z}_{\tau|k}^\mu$ for each pair $(\tau, \pi^\mu) \in \{0, \dots, T_\phi\} \times \mathcal{P}$. We note that this assignment is potentially non-unique. Specifically, let $\bar{z}_{\tau|k}^\mu = 1$ for all pairs $(\tau, \pi^\mu) \in TP_k$, where $TP_k \subseteq \{1, \dots, T_\phi\} \times \mathcal{P}$, and let $\bar{z}_{\tau|k}^\mu = 0$ otherwise. For each pair $(\tau, \pi^\mu) \in TP_k$ such that $\bar{z}_{\tau|k}^\mu = 1$, we further know by equations (19) and (20) that there exists at least one $s \in \{0, \dots, k\}$ such that $q_{\tau|k}^{\mu,s} = 1$. If it holds that $Y_{k+1} \in \mathcal{B}_{k+1|s}$ for all $s \in \{0, \dots, k\}$, which holds with probability $1 - \delta$ due to Theorem 5, then we have a feasible solution $\mathbf{u}_{k+1} := u_{k+1|k}^*, \dots, u_{T_\phi-1|k}^*$ of the optimization problem (14) at the next time step $k + 1$. This holds for the following reasons:

- For $\tau \leq k$, we have $\bar{z}_{\tau|k+1}^\mu = \bar{z}_{\tau|k}^\mu = 1$ for all $(\tau, \pi^\mu) \in TP_k$ since the states x_τ and Y_τ were known already;
- For $\tau = k + 1$, we have $\bar{z}_{\tau|k+1}^\mu = \bar{z}_{\tau|k}^\mu = 1$ for all $(\tau, \pi^\mu) \in TP_k$ due to the minimum operation in (19) if $Y_{k+1} \in \mathcal{B}_{k+1|s}$ for all $s \in \{0, \dots, k\}$, which again holds with probability $1 - \delta$ due to Theorem 5;
- For $\tau \geq k + 2$, we have $\bar{z}_{\tau|k+1}^\mu = \bar{z}_{\tau|k}^\mu = 1$ for all $(\tau, \pi^\mu) \in TP_k$ since (19) and (20) hold at time step $k + 1$ for $x_{\tau|k+1} = x_{\tau|k}$ (obtained by applying the controller \mathbf{u}_{k+1}) and for $q_{\tau|k+1}^{\mu,s} = q_{\tau|k}^{\mu,s}$.

Using the fact that ϕ is in positive normal form, these observations imply that \mathbf{u}_{k+1} is a feasible solution of the optimization problem (14) with $\bar{z}_{0|k+1}^\phi = 1$ at time $k + 1$ if $\bar{z}_{0|k}^\phi = 1$ and if $Y_{k+1} \in \mathcal{B}_{k+1|s}$ for all $s \in \{0, \dots, k\}$, which holds with probability $1 - \delta$ due to Theorem 5.

We can repeat the previous reasoning for all T_ϕ time steps, i.e., we can ensure recursive feasibility at each time $k \in \{1, \dots, T_\phi - 1\}$ if it holds that $Y_k \in \mathcal{B}_{k|s}$ for all $k \in \{1, \dots, T_\phi - 1\}$ and $s \in \{0, \dots, k - 1\}$. Due Theorem 5, we thus know that the probability of (14) being feasible at every time step $k \in \{1, \dots, T_\phi - 1\}$ is larger than or equal to $1 - \delta$, which completes the first part of the proof.

At time step $k = T_\phi - 1$, $\bar{z}_{0|k}^\phi = 1$ implies $\bar{z}_{0|k+1}^\phi = 1$ with probability $1 - \delta$ due to the recursive feasibility as above. This means that the trajectory $s_0 s_1 \dots s_{T_\phi}$ will satisfy ϕ with probability $1 - \delta$, which completes the second part of the proof - probabilistic task satisfaction. \square

6 Case studies

In this section, we illustrate our control method on two case studies. All simulations are conducted in Python 3 and we use SCIP [68] to solve the optimization problem. Our implementations are available at <https://github.com/SAIDS-Lab/STL-Synthesis-among-Uncontrollable-Agents>, where more details can be found.

6.1 Building temperature control

We consider the temperature control of a public space in a hall with floor plan shown in Figure 2. Specifically, we can control the temperature of Room 1, which is the public space, while Rooms 2 and 3 are uncontrollable for us, e.g., these may be meeting rooms where the temperature can only be adjusted manually. Formally, the dynamics of the system are given as

$$x_{k+1} = x_k + \tau_s(\alpha_e(T_e - x_k) + \alpha_H(T_h - x_k)u_k),$$

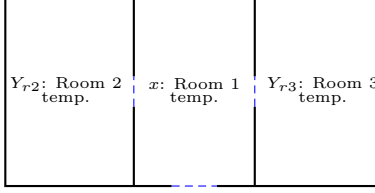


Figure 2: The floor plan of the hall.

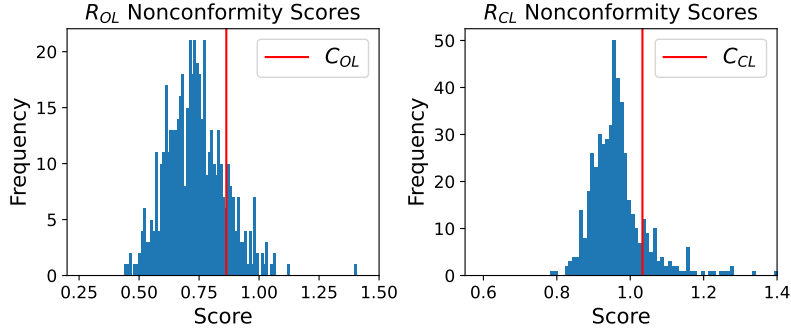


Figure 3: Nonconformity scores $R_{OL}^{(j)}$ (left) and $R_{CL}^{(j)}$ (right) on D_{cal} in the temperature control case.

where the state $x_k \in \mathcal{X} = [0, 45]$ denotes the temperature of the public space at time k , the control input $u_k \in \mathcal{U} = [0, 1]$ is the ratio of the heater valve, τ_s is the sampling time for the discrete dynamics, $T_h = 55^\circ C$ is the heater temperature, $T_e = 5^\circ C$ is the outside temperature, and $\alpha_e = 0.06$ and $\alpha_H = 0.08$ are heat exchange coefficients. The initial state is $x_0 = 5$. The model is adopted from [39].

System Specification. The task is to ensure that the difference between the temperatures in the public space and the two meeting rooms is bounded, e.g., such that during transition between rooms people feel comfortable. Let $Y_{r,2}$ and $Y_{r,3}$ denote the uncontrollable random variables describing the temperatures of Rooms 2 and 3. In particular, we require that, the difference between x and the temperatures of $Y_{r,2}$ and $Y_{r,3}$ should be below a threshold of $5^\circ C$ for at least an hour starting from within the first 4 minutes. We set the sampling time to be $\tau_s = 2$ minutes, and we

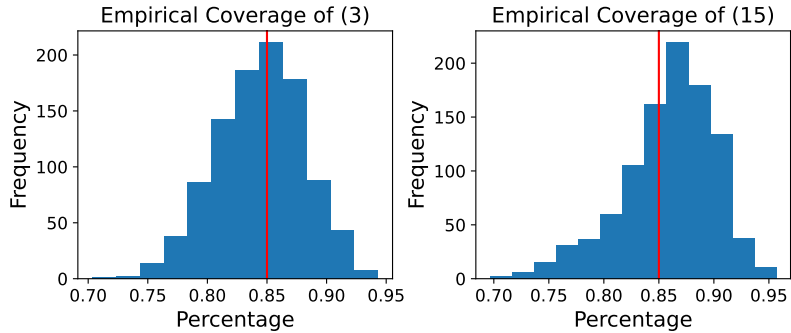


Figure 4: Empirical validation results about the coverage of $R_{OL}^{(j)} \leq C_{OL}$ (left) and $R_{CL}^{(j)} \leq C_{CL}$ (right) in the temperature control case.

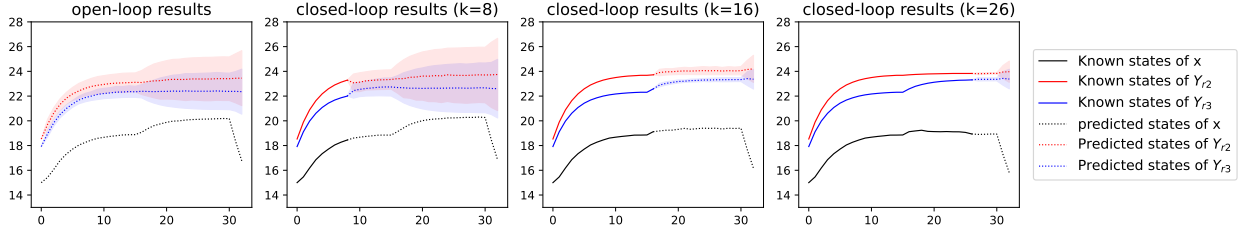


Figure 5: The result of the temperature qualitative control of the first case study.

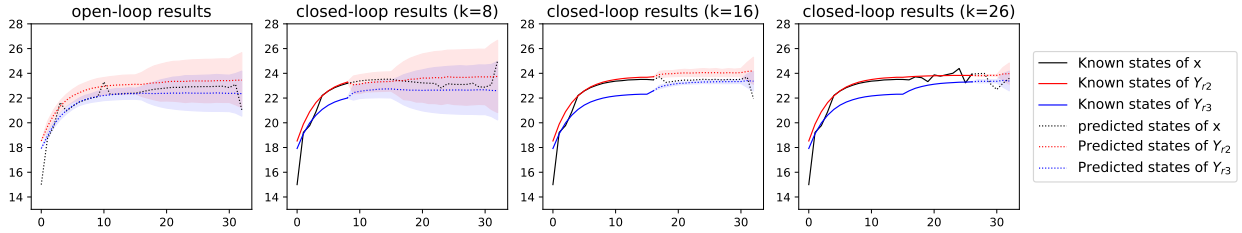


Figure 6: The result of the temperature quantitative control of the first case study.

describe the task as follows:

$$\phi := \mathbf{F}_{[0,2]} \mathbf{G}_{[0,30]} (x - Y_{r2} \leq 5 \wedge x - Y_{r2} \geq -5 \wedge x - Y_{r3} \leq 5 \wedge x - Y_{r3} \geq -5).$$

In this case, we set the failure probability to be 15%, i.e., $\delta := 0.15$.

Behavior of uncontrollable rooms. The group of people will adjust the temperature in the rooms based on their individual temperature preferences when they enter the meeting room. We assume the temperature variation in Y_{r2} and Y_{r3} generated by this adjustment is described by Newton’s Law of Cooling [69].

Data Collection. We collected 2000 trajectories of temperature trajectories for Rooms 2 and 3 – generated as described before. We split them into training (used for the trajectory predictor), calibration (used for conformal prediction), and test (used for validation) datasets with sizes $|D_{train}| = 500$, $|D_{cal}| = 500$ and $|D_{test}| = 1000$, respectively. From the training data D_{train} , we train a long-short-term memory (LSTM) network to make predictions about the room temperature. We note that we warm-start the LSTM at time $k = 0$ with data, e.g., the LSTM is fed with past information y_{-6}, \dots, y_{-1} .

Multi-agent prediction regions. Fig. 3 shows histograms of the nonconformity scores $R_{OL}^{(j)}$ and $R_{CL}^{(j)}$ evaluated on D_{cal} . From these histograms of nonconformity scores, we compute $C_{OL} := 0.863$ and $C_{CL} := 1.033$ according to Theorems 1 and 5. Next, we empirically validate the correctness of the prediction regions in (3) and (15). We perform the following two experiments 1000 times each. In the first experiment, we randomly sample 150 calibration trajectories from D_{cal} and 150 test trajectories from D_{test} . Then, we construct C_{OL} and C_{CL} from the 150 calibration trajectories and compute the ratio of how many of the 150 test trajectories satisfy $R_{OL}^{(j)} \leq C_{OL}$ and $R_{CL}^{(j)} \leq C_{CL}$, respectively. Fig. 4 shows the histogram over these ratios, and we can observe that the result achieves the desired coverage $1 - \delta = 0.85$. In the second experiment, we randomly sample 150 calibration trajectories from D_{cal} and 1 test trajectories from D_{test} . Then, we construct

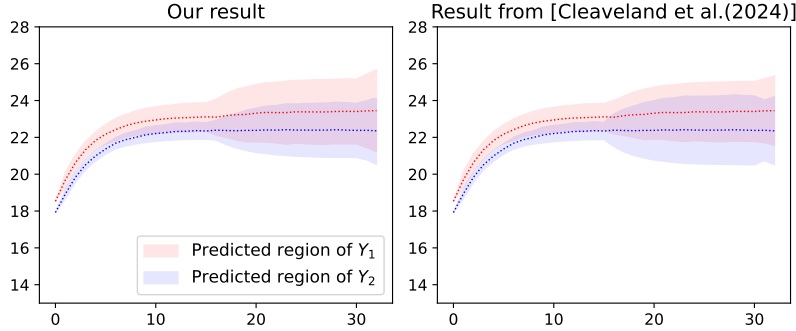


Figure 7: The comparison result of the open-loop prediction regions of the first case study.

C_{OL} and C_{CL} from the 150 calibration trajectories and check whether or not the sampled test data satisfies $R_{OL}^{(j)} \leq C_{OL}$ and $R_{CL}^{(j)} \leq C_{CL}$, respectively. We find a ratio of 0.913 for $R_{OL}^{(j)} \leq C_{OL}$ and a ratio of 0.871 for $R_{CL}^{(j)} \leq C_{CL}$, respectively, which further empirically confirms (3) and (15). For one of these test trajectories, Fig. 5 shows the prediction regions by shaded areas defined by $\hat{Y}_{\tau|k}$ and $C_{\tau|k}$ for $\tau > k$ where $k = 0, k = 8, k = 16$ and $k = 26$ from the left to the right, respectively.

Prediction region comparison. We compare our method with [62], where a parameterized prediction error was proposed. Instead of computing the maximum prediction error σ as in (4) and (16), they proposed an optimization-based method to obtain an in some sense optimal σ that results in small prediction regions (see [62] for details). Specifically, they formulate the problem as a mixed integer linear complementarity program (MILCP). We extend their framework to the multi-agent case and solve the optimization problem with CasADI [70]. The result is shown in Fig. 7. Our computation time is 0.007s, much less than theirs, which is 2.82s. Furthermore, the shape of the region looks similar. It is worth mentioning that although they claim they can find the smallest prediction region theoretically, it is sometimes difficult to realize this in practice due to nonconvexity of the optimization problem.

Qualitative predictive control synthesis. We run the open-loop and closed-loop control frameworks 1000 times with data from D_{test} , respectively, where the cost function is set to be the minimum summation of squared control inputs as $J := \sum_{k=0}^{31} u_k^2$. In the open-loop control case, the problem is feasible for 1000 times, where the average computation time, average robustness, and task satisfaction rate⁴ are 0.148s, 0.15, and 0.955, respectively. In the closed-loop control case, the problem is feasible at the initial time $k = 0$ for 999 times⁵, and recursive feasibility is achieved for 986 times, where the average total computation time, average robustness, and task satisfaction rate are 5.90s, 0.07, and 0.987, respectively. We remark that the closed-loop controller has slightly lower robustness than the open-loop controller. This is since the closed-loop prediction regions $\mathcal{B}_{\tau|k}$ for large k appear to be less conservative than open-loop prediction regions. We also see that the closed-loop controller has a higher task satisfaction rate since the controller can update the control inputs in a receding horizon fashion to observations of the uncontrollable agents. Fig. 5 shows one of the results of the proposed control framework with the qualitative encoding. Fig. 5(a) specifically presents the result of the open loop controller where the prediction regions are large for large τ , while Figs. 5(b)(c)(d) present the result of the closed loop controller at times $k = 8, 16, 26$,

⁴The task satisfaction rate is computed as the ratio between the number of times ϕ is satisfied and the number of times the optimization problem is feasible at time $k = 0$.

⁵We note the difference in initial feasibility compared to the open-loop controller, which is caused since prediction regions $\mathcal{B}_{\tau|0}$ of the closed-loop controller are more conservative.

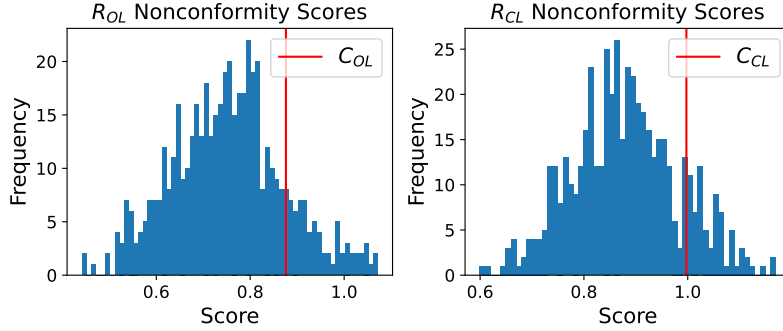


Figure 8: Nonconformity scores $R_{OL}^{(j)}$ (left) and $R_{CL}^{(j)}$ (right) on D_{cal} in the robot motion planning case.

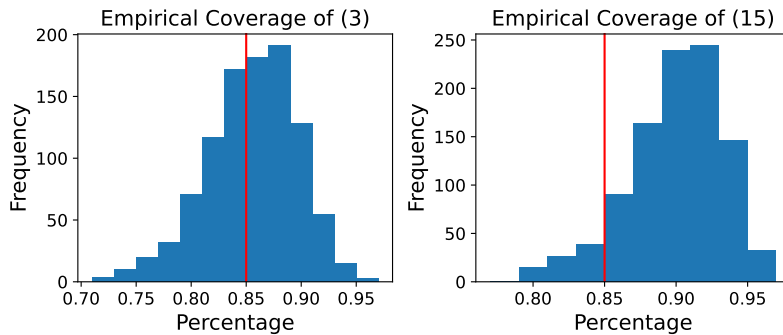


Figure 9: Empirical validation results about the coverage of $R_{OL}^{(j)} \leq C_{OL}$ (left) and $R_{CL}^{(j)} \leq C_{CL}$ (right) in the robot motion planning case.

respectively.

Quantitative predictive control synthesis. Similar to the qualitative control, we run the open-loop and closed-loop control frameworks with quantitative encoding 1000 times with data in D_{test} , respectively, where we enforce the robust semantics to be larger than 1, i.e., $\bar{r}_{0|k}^\phi \geq 0$, and we maximize $\bar{r}_{0|k}^\phi$ in the cost function, i.e., we set $J := -\bar{r}_{0|k}^\phi$. In the open-loop control case, the problem is feasible for 927 times, where the average computation time, average robustness, and task satisfaction rate are 1.79s, 2.92, and 1, respectively. In the closed-loop control case, the problem is feasible at the initial time $k = 0$ for 923 times, and the recursive feasibility is achieved for 890 times, where the average computation time, average robustness, and task satisfaction rate are 147.29s, 2.80, and 0.964, respectively. The closed-loop controller has a lower task satisfaction rate than the open-loop controller due to the nonconvexity of the optimization problem and performance issues of our solver in practice. It is worthy noting that the computation time of the quantitative encoding is greater than that of the qualitative encoding, although it may achieve better robustness performance. As we can see in the result in Fig. 6, the trajectory stays near the center of the prediction regions, leading to higher robustness.

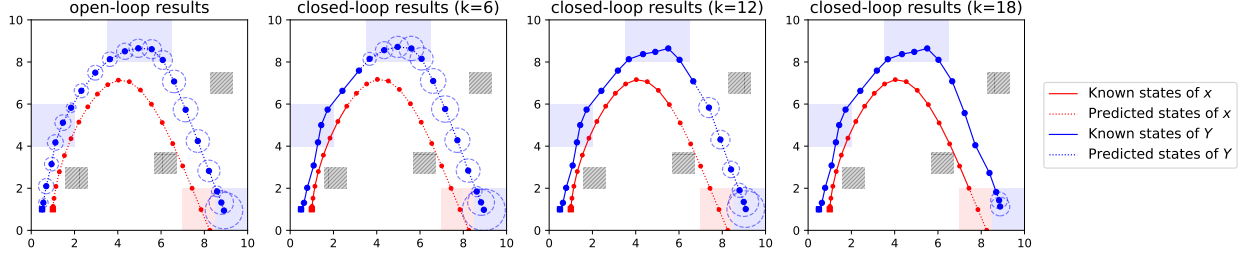


Figure 10: The result of the robot motion planning of the second case study.

6.2 Robot motion planning

We consider the planar motion of a single robot (denoted by R_1) with double integrator dynamics. The system model, with a sampling period of 1 second, is described as

$$x_{k+1} = \begin{bmatrix} 1 & 1 & 0 & 0 \\ 0 & 1 & 0 & 0 \\ 0 & 0 & 1 & 1 \\ 0 & 0 & 0 & 1 \end{bmatrix} x_k + \begin{bmatrix} 0.5 & 0 \\ 1 & 0 \\ 0 & 0.5 \\ 0 & 1 \end{bmatrix} u_k,$$

where the state $x_k = [p_x^1 \ v_x^1 \ p_y^1 \ v_y^1]^\top$ denotes the x -position, x -velocity, y -position and y -velocity, and where the control input $u_k = [u_x \ u_y]^\top$ denotes the x -acceleration and y -acceleration, respectively. The physical constraints are $x \in \mathcal{X} = [0, 10] \times [-1.5, 1.5] \times [0, 10] \times [-1.5, 1.5]$ and $u \in \mathcal{U} = [-1, 1] \times [-1, 1]$. The initial state is $x_0 = [1, 0, 1, 0]^\top$. Furthermore, we have one more uncontrollable agent (denoted by R_2) and its state $Y_k = [P_x^2 \ P_y^2]^\top$ denotes the x -position and y -position. Then we define the joint state as $s_k = [p_x^1 \ v_x^1 \ p_y^1 \ v_y^1 \ P_x^2 \ P_y^2]^\top$. In this case, R_1 is controllable and R_2 is uncontrollable.

System Specification. The objective of the two robots is to visit specific regions to perform specific tasks, such as collecting packages and transporting them to a final destination. For this collaborative task, R_2 is the leader and R_1 should follow R_2 . Specifically, R_2 should arrive and stay in the left blue region and top blue region, as shown in the Fig. 10, within the time intervals $[4, 6]$ and $[9, 13]$, respectively. After that, starting from a certain time instant between the time interval $[16, 18]$, R_1 and R_2 should stay in bottom right red and blue regions respectively for at least 2 time instants. During the task execution, the distances between the two agents should be at most D meters such that the two robots can communicate or perform collaborative tasks. Furthermore, the two robots should always avoid the obstacles (grey shaded areas). In particular, such a task can be described by the following formula:

$$\phi := \mathbf{G}_{[4,6]} \pi^{\mu_1} \wedge \mathbf{G}_{[9,13]} \pi^{\mu_2} \wedge \mathbf{F}_{[16,18]} \mathbf{G}_{[0,2]} (\pi^{\mu_3} \wedge \pi^{\mu_4}) \wedge \mathbf{G}_{[0,20]} (\pi^{\mu_{close}} \wedge \pi^{\mu_{obs1}} \wedge \pi^{\mu_{obs2}}),$$

where $\mu_1 := \min(P_x^2 - 2, 2 - P_x^2, P_y^2 - 4, 6 - P_y^2)$, $\mu_2 := \min(P_x^2 - 3.5, 6.5 - P_x^2, P_y^2 - 8, 10 - P_y^2)$, $\mu_3 := \min(P_x^2 - 8.5, 10 - P_x^2, P_y^2 - 2 - P_y^2)$ and $\mu_4 := \min(p_x^1 - 7, 8.5 - p_x^1, p_y^1 - 2 - P_y^1)$ represent the tasks for R_2 in the left blue region, R_2 in the top blue region, R_2 in the bottom right blue region, and R_1 in the bottom red region, respectively. Here, $\mu_{close} := D - \min(P_x^2 - p_x^1, p_x^1 - P_x^2, P_y^2 - p_y^1, p_y^1 - P_y^2)$ is the predicate regarding the distance requirement between the two robots where we set $D = 2$. The predicates $\mu_{obs1} := \min(\max(1.6 - p_x^1, p_x^1 - 2.6, 2 - p_y^1, p_y^1 - 3), \max(8.3 - p_x^1, p_x^1 - 9.3, 6.5 - p_y^1, p_y^1 - 7.5), \max(5.7 - p_x^1, p_x^1 - 6.7, 2.7 - p_y^1, p_y^1 - 3.7))$ and $\mu_{obs2} := \min(\max(1.6 - P_x^2, P_x^2 - 2.6, 2 -$

$P_y^2, P_y^2 - 3$), $\max(8.3 - P_x^2, P_x^2 - 9.3, 6.5 - P_y^2, P_y^2 - 7.5)$, $\max(5.7 - P_x^2, P_x^2 - 6.7, 2.7 - P_y^2, P_y^2 - 3.7)$) describe the tasks for obstacle avoidance. From an individual robot perspective, we can decompose ϕ into two task for each of the two robots as follows

$$\begin{aligned}\phi_{R_1} &:= \mathbf{F}_{[16,18]} \mathbf{G}_{[0,2]} \pi^{\mu_4} \wedge \mathbf{G}_{[0,20]} (\pi^{\mu_{close}} \wedge \pi^{\mu_{obs1}}), \\ \phi_{R_2} &:= \mathbf{G}_{[4,6]} \pi^{\mu_1} \wedge \mathbf{G}_{[9,13]} \pi^{\mu_2} \wedge \mathbf{F}_{[16,18]} \mathbf{G}_{[0,2]} \pi^{\mu_3} \wedge \mathbf{G}_{[0,20]} \pi^{\mu_{obs2}}.\end{aligned}$$

As R_2 will lead the task, its behavior will not be influenced by R_1 . On the other hand, R_1 is responsible for the task μ_{close} which means it should always track the behavior of R_2 . Regarding the execution of the task, we only enforce R_1 to achieve ϕ_{R_1} instead of ϕ , which makes sense in the leader-follower setting of this case study.

Motion of uncontrollable agent. The motion of the uncontrollable agent R_2 is described as follows. We set its dynamical system as $y_{k+1} = f(y_k, u_k^y) + \omega_k$ where $f(y_k, u_k^y)$ describes the same double integrator dynamics as for R_1 , and $\omega_k \in \mathcal{W}$ is a uniformly distributed disturbance from the set $\mathcal{W} = ([-0.15, 0.15] \times [0, 0])^2$. We compute an closed-loop control sequence for R_2 under the specification ϕ_{R_2} using a standard MIP encoding [27].

Data collection. We collected 2000 trajectories of the uncontrollable agent. We split the data into training, calibration, and test datasets with sizes $|D_{train}| = 500$, $|D_{cal}| = 500$ and $|D_{test}| = 1000$, respectively. We again trained an LSTM on D_{train} for trajectory prediction.

Prediction regions. Fig. 8 shows histograms of the nonconformity scores $R_{OL}^{(j)}$ and $R_{CL}^{(j)}$ evaluated on D_{cal} . Based on these nonconformity scores, we have that $C_{OL} = 0.876$ and $C_{CL} = 0.997$ by using $\delta = 0.15$. Next, we empirically validate the correctness of the prediction regions by checking whether or not (3) and (15) hold on D_{test} by the same two experiments as the temperature control case. Fig. 9 shows the histogram over the result of the ratios in the first experiment, and we can observe that the result achieves the desired coverage $1 - \delta = 0.85$. In the second experiment, we obtain a ratio of 0.854 for $R_{OL}^{(j)} \leq C_{OL}$ and a ratio of 0.894 for $R_{CL}^{(j)} \leq C_{CL}$, respectively, which also empirically confirms (3) and (15). For one of these test trajectories, Fig. 10 shows the prediction regions defined by $\hat{Y}_{\tau|k}$ and $C_{\tau|k}$ for $\tau > k$ where $k = 0$, $k = 6$, $k = 12$ and $k = 18$, respectively.

Predictive control synthesis. As in our first experiment, we run the open-loop and the closed-loop controller with the qualitative encoding 1000 times with data from D_{test} . The cost function encodes the trade off between the sum of the squared control inputs and velocities as $J := \sum_{k=0}^{20} (0.97 \|u_k\|^2 + 0.03 (v_x^1)^2 + 0.03 (v_y^1)^2)$. In the open-loop control case, the problem is feasible for 1000 times, where the average computation time, average robustness, and task satisfaction rate are 0.70s, 0.06490, and 1, respectively. In the closed-loop control case, the problem is feasible at the initial time $k = 0$ for 1000 times, with recursive feasibility in all cases, where the average total computation time, average robustness, and task satisfaction rate are 14.80s, 0.06489, and 1, respectively. The closed-loop case has again a slightly lower robustness for the same reasons as in the first experiment. Fig. 10 shows one of the results of the proposed control framework, where we can see that robot R_1 will use the prediction regions of R_2 to compute a control input that results in task satisfaction. Fig. 10(a) specifically presents the result of the open loop controller while Figs. 10(b)(c)(d) present the result of the closed loop controller at times $k = 6, 12, 18$, respectively.

7 Conclusion

In this paper, we presented a control framework for signal temporal logic (STL) control synthesis where the STL specification is defined over the dynamical system and uncontrollable dynamic agents. We use trajectory predictors and conformal prediction to provide prediction regions for

the uncontrollable agents that are valid with high probability. Then, we formulated predictive open-loop control laws that consider the worst case realization of the uncontrollable agents within the prediction region. Specifically, we proposed a mixed integer program (MIP) that results in the probabilistic satisfaction of the STL specification, and we presented an equivalent MIP program based on the KKT conditions of the original MIP program to obtain more efficient solutions. Finally, we presented a probabilistic recursively feasible closed-loop control framework that can provide high probability guarantee for the task satisfaction. We provided two case studies for temperature control and robot motion planning, and we demonstrated the correctness and efficiency of our control framework.

References

- [1] M. Guo and D. Dimarogonas, “Multi-agent plan reconfiguration under local LTL specifications,” *The International Journal of Robotics Research*, vol. 34, no. 2, pp. 218–235, 2015.
- [2] M. Kloetzer and C. Belta, “Automatic deployment of distributed teams of robots from temporal logic motion specifications,” *IEEE Transactions on Robotics*, vol. 26, no. 1, pp. 48–61, 2009.
- [3] Y. Kantaros and M. Zavlanos, “Stylus*: A temporal logic optimal control synthesis algorithm for large-scale multi-robot systems,” *The International Journal of Robotics Research*, vol. 39, no. 7, pp. 812–836, 2020.
- [4] D. Sun, J. Chen, S. Mitra, and C. Fan, “Multi-agent motion planning from signal temporal logic specifications,” *IEEE Robotics and Automation Letters*, vol. 7, no. 2, pp. 3451–3458, 2022.
- [5] Y. Kantaros, M. Guo, and M. Zavlanos, “Temporal logic task planning and intermittent connectivity control of mobile robot networks,” *IEEE Transactions on Automatic Control*, vol. 64, no. 10, pp. 4105–4120, 2019.
- [6] A. Büyükköçak, D. Aksaray, and Y. Yazicioglu, “Distributed planning of multi-agent systems with coupled temporal logic specifications,” in *AIAA Scitech 2021 Forum*, p. 1123, 2021.
- [7] L. Lindemann and D. Dimarogonas, “Control barrier functions for multi-agent systems under conflicting local signal temporal logic tasks,” *IEEE control systems letters*, vol. 3, no. 3, pp. 757–762, 2019.
- [8] M. Srinivasan, S. Coogan, and M. Egerstedt, “Control of multi-agent systems with finite time control barrier certificates and temporal logic,” in *IEEE Conference on Decision and Control*, pp. 1991–1996, IEEE, 2018.
- [9] S. Kalluraya, G. Pappas, and Y. Kantaros, “Multi-robot mission planning in dynamic semantic environments,” in *IEEE International Conference on Robotics and Automation*, pp. 1630–1637, IEEE, 2023.
- [10] B. Hoxha and G. Fainekos, “Planning in dynamic environments through temporal logic monitoring,” in *AAAI Workshop: Planning for Hybrid Systems*, vol. 16, p. 12, 2016.
- [11] Y. Li, E. Shahrivar, and J. Liu, “Safe linear temporal logic motion planning in dynamic environments,” in *IEEE/RSJ International Conference on Intelligent Robots and Systems*, pp. 9818–9825, IEEE, 2021.

- [12] M. Kloetzer and C. Mahulea, “LTL planning in dynamic environments,” *IFAC Proceedings Volumes*, vol. 45, no. 29, pp. 294–300, 2012.
- [13] A. Ulusoy and C. Belta, “Receding horizon temporal logic control in dynamic environments,” *The International Journal of Robotics Research*, vol. 33, no. 12, pp. 1593–1607, 2014.
- [14] A. Ayala, S. Andersson, and C. Belta, “Temporal logic control in dynamic environments with probabilistic satisfaction guarantees,” in *IEEE/RSJ International Conference on Intelligent Robots and Systems*, pp. 3108–3113, IEEE, 2011.
- [15] P. Purohit and I. Saha, “Dt: Temporal logic path planning in a dynamic environment,” in *IEEE/RSJ International Conference on Intelligent Robots and Systems*, pp. 3627–3634, IEEE, 2021.
- [16] L. Lindemann, M. Cleaveland, G. Shim, and G. Pappas, “Safe planning in dynamic environments using conformal prediction,” *IEEE Robotics and Automation Letters*, 2023.
- [17] A. Dixit, L. Lindemann, S. Wei, M. Cleaveland, G. Pappas, and J. Burdick, “Adaptive conformal prediction for motion planning among dynamic agents,” in *Learning for Dynamics and Control Conference*, pp. 300–314, PMLR, 2023.
- [18] S. Tonkens, S. Sun, R. Yu, and S. Herbert, “Scalable safe long-horizon planning in dynamic environments leveraging conformal prediction and temporal correlations,” 2023.
- [19] A. Muthali, H. Shen, S. Deglurkar, M. Lim, R. Roelofs, A. Faust, and C. Tomlin, “Multi-agent reachability calibration with conformal prediction,” in *IEEE Conference on Decision and Control*, pp. 6596–6603, IEEE, 2023.
- [20] O. Maler and D. Nickovic, “Monitoring temporal properties of continuous signals,” in *Conference on Formal Techniques, Modelling and Analysis of Timed and Fault Tolerant Systems*, pp. 152–166, Springer, 2004.
- [21] G. Fainekos and G. Pappas, “Robustness of temporal logic specifications for continuous-time signals,” *Theoretical Computer Science*, vol. 410, no. 42, pp. 4262–4291, 2009.
- [22] A. Donzé and O. Maler, “Robust satisfaction of temporal logic over real-valued signals,” in *International Conference on Formal Modeling and Analysis of Timed Systems*, pp. 92–106, Springer, 2010.
- [23] Y. V. Pant, H. A., and R. Mangharam, “Smooth operator: Control using the smooth robustness of temporal logic,” in *IEEE Conference on Control Technology and Applications*, pp. 1235–1240, IEEE, 2017.
- [24] Y. Pant, H. Abbas, R. Quaye, and R. Mangharam, “Fly-by-logic: Control of multi-drone fleets with temporal logic objectives,” in *ACM/IEEE International Conference on Cyber-Physical Systems*, pp. 186–197, IEEE, 2018.
- [25] N. Mehdipour, C. Vasile, and C. Belta, “Arithmetic-geometric mean robustness for control from signal temporal logic specifications,” in *American Control Conference*, pp. 1690–1695, 2019.
- [26] Y. Gilpin, V. Kurtz, and H. Lin, “A smooth robustness measure of signal temporal logic for symbolic control,” *IEEE Control Systems Letters*, vol. 5, no. 1, pp. 241–246, 2020.

- [27] V. Raman, A. Donzé, M. Maasoumy, R. Murray, A. Sangiovanni-Vincentelli, and S. Seshia, “Model predictive control with signal temporal logic specifications,” in *53rd IEEE Conference on Decision and Control*, pp. 81–87, IEEE, 2014.
- [28] S. Sadraddini and C. Belta, “Formal synthesis of control strategies for positive monotone systems,” *IEEE Transactions on Automatic Control*, vol. 64, no. 2, pp. 480–495, 2018.
- [29] V. Kurtz and H. Lin, “Mixed-integer programming for signal temporal logic with fewer binary variables,” *IEEE Control Systems Letters*, vol. 6, pp. 2635–2640, 2022.
- [30] L. Lindemann and D. Dimarogonas, “Control barrier functions for signal temporal logic tasks,” *IEEE control systems letters*, vol. 3, no. 1, pp. 96–101, 2018.
- [31] M. Charitidou and D. Dimarogonas, “Receding horizon control with online barrier function design under signal temporal logic specifications,” *IEEE Transactions on Automatic Control*, 2022.
- [32] W. Xiao, C. Belta, and C. Cassandras, “High order control lyapunov-barrier functions for temporal logic specifications,” in *2021 American Control Conference (ACC)*, pp. 4886–4891, IEEE, 2021.
- [33] S. Farahani, R. Majumdar, V. Prabhu, and S. Soudjani, “Shrinking horizon model predictive control with chance-constrained signal temporal logic specifications,” in *American Control Conference*, pp. 1740–1746, 2017.
- [34] S. Jha, V. Raman, D. Sadigh, and S. Seshia, “Safe autonomy under perception uncertainty using chance-constrained temporal logic,” *Journal of Automated Reasoning*, vol. 60, pp. 43–62, 2018.
- [35] D. Sadigh and A. Kapoor, “Safe control under uncertainty with probabilistic signal temporal logic,” in *Proceedings of Robotics: Science and Systems XII*, 2016.
- [36] R. Ilyes, Q. Ho, and M. Lahijanian, “Stochastic robustness interval for motion planning with signal temporal logic,” in *IEEE International Conference on Robotics and Automation*, pp. 5716–5722, IEEE, 2023.
- [37] C. Vasile, V. Raman, and S. Karaman, “Sampling-based synthesis of maximally-satisfying controllers for temporal logic specifications,” in *2017 IEEE/RSJ International Conference on Intelligent Robots and Systems (IROS)*, pp. 3840–3847, IEEE, 2017.
- [38] G. Scher, S. Sadraddini, A. Yadin, and H. Kress-Gazit, “Ensuring reliable robot task performance through probabilistic rare-event verification and synthesis,” *arXiv preprint arXiv:2304.14886*, 2023.
- [39] P. Jagtap, S. Soudjani, and M. Zamani, “Formal synthesis of stochastic systems via control barrier certificates,” *IEEE Transactions on Automatic Control*, vol. 66, no. 7, pp. 3097–3110, 2020.
- [40] S. Safaoui, L. Lindemann, D. Dimarogonas, I. Shames, and T. Summers, “Control design for risk-based signal temporal logic specifications,” *IEEE Control Systems Letters*, vol. 4, no. 4, pp. 1000–1005, 2020.

- [41] P. Akella, A. Dixit, M. Ahmadi, J. W. Burdick, and A. D. Ames, “Sample-based bounds for coherent risk measures: Applications to policy synthesis and verification,” *Artificial Intelligence*, p. 104195, 2024.
- [42] N. Hashemi, X. Qin, J. Deshmukh, G. Fainekos, B. Hoxha, D. Prokhorov, and T. Yamaguchi, “Risk-awareness in learning neural controllers for temporal logic objectives,” in *American Control Conference*, pp. 4096–4103, IEEE, 2023.
- [43] L. Lindemann, G. Pappas, and D. Dimarogonas, “Reactive and risk-aware control for signal temporal logic,” *IEEE Transactions on Automatic Control*, vol. 67, no. 10, pp. 5262–5277, 2021.
- [44] D. Gundana and H. Kress-Gazit, “Event-based signal temporal logic synthesis for single and multi-robot tasks,” *IEEE Robotics and Automation Letters*, vol. 6, no. 2, pp. 3687–3694, 2021.
- [45] D. Gundana and H. Kress-Gazit, “Event-based signal temporal logic tasks: Execution and feedback in complex environments,” *IEEE Robotics and Automation Letters*, vol. 7, no. 4, pp. 10001–10008, 2022.
- [46] V. Raman, A. Donzé, D. Sadigh, R. Murray, and S. Seshia, “Reactive synthesis from signal temporal logic specifications,” in *international conference on hybrid systems: Computation and control*, pp. 239–248, 2015.
- [47] G. Shafer and V. Vovk, “A tutorial on conformal prediction.,” *Journal of Machine Learning Research*, vol. 9, no. 3, 2008.
- [48] V. Vovk, A. Gammerman, and G. Shafer, *Algorithmic learning in a random world*, vol. 29. Springer, 2005.
- [49] A. Angelopoulos and S. Bates, “A gentle introduction to conformal prediction and distribution-free uncertainty quantification,” *arXiv preprint arXiv:2107.07511*, 2021.
- [50] M. Fontana, G. Zeni, and S. Vantini, “Conformal prediction: a unified review of theory and new challenges,” *Bernoulli*, vol. 29, no. 1, pp. 1–23, 2023.
- [51] M. Cauchois, S. Gupta, A. Ali, and J. Duchi, “Robust validation: Confident predictions even when distributions shift,” *Journal of the American Statistical Association*, pp. 1–66, 2024.
- [52] I. Gibbs and E. Candes, “Adaptive conformal inference under distribution shift,” *Advances in Neural Information Processing Systems*, vol. 34, pp. 1660–1672, 2021.
- [53] A. Donzé and O. Maler, “Robust satisfaction of temporal logic over real-valued signals,” in *Formal Modeling and Analysis of Timed Systems*, pp. 92–106, 2010.
- [54] A. Dokhanchi, B. Hoxha, and G. Fainekos, “On-line monitoring for temporal logic robustness,” in *Runtime Verification*, pp. 231–246, Springer, 2014.
- [55] S. Sadraddini and C. Belta, “Robust temporal logic model predictive control,” in *Annual Allerton Conference on Communication, Control, and Computing*, pp. 772–779, IEEE, 2015.
- [56] H. Salehinejad, S. Sankar, J. Barfett, E. Colak, and S. Valaee, “Recent advances in recurrent neural networks,” *arXiv preprint arXiv:1801.01078*, 2017.

- [57] Y. Yu, X. Si, C. Hu, and J. Zhang, “A review of recurrent neural networks: Lstm cells and network architectures,” *Neural computation*, vol. 31, no. 7, pp. 1235–1270, 2019.
- [58] K. Han, A. Xiao, E. Wu, J. Guo, C. Xu, and Y. Wang, “Transformer in transformer,” *Advances in Neural Information Processing Systems*, vol. 34, pp. 15908–15919, 2021.
- [59] R. Tibshirani, R. Foygel Barber, E. Candes, and A. Ramdas, “Conformal prediction under covariate shift,” *Advances in neural information processing systems*, vol. 32, 2019.
- [60] K. Stankeviciute, A. M Alaa, and M. van der Schaar, “Conformal time-series forecasting,” *Advances in neural information processing systems*, vol. 34, pp. 6216–6228, 2021.
- [61] Y. Zhao, B. Hoxha, G. Fainekos, J. Deshmukh, and L. Lindemann, “Robust conformal prediction for stl runtime verification under distribution shift,” in *ACM/IEEE International Conference on Cyber-Physical Systems*, pp. 169–179, IEEE, 2024.
- [62] M. Cleaveland, I. Lee, G. Pappas, and L. Lindemann, “Conformal prediction regions for time series using linear complementarity programming,” in *AAAI Conference on Artificial Intelligence*, vol. 38, pp. 20984–20992, 2024.
- [63] I. Gibbs, J. Cherian, and E. Candès, “Conformal prediction with conditional guarantees,” *arXiv preprint arXiv:2305.12616*, 2023.
- [64] A. Bemporad and M. Morari, “Control of systems integrating logic, dynamics, and constraints,” *Automatica*, vol. 35, no. 3, pp. 407–427, 1999.
- [65] S. Boyd and L. Vandenberghe, *Convex optimization*. Cambridge university press, 2004.
- [66] L. Lindemann, X. Qin, J. V. Deshmukh, and G. Pappas, “Conformal prediction for STL runtime verification,” in *ACM/IEEE International Conference on Cyber-Physical Systems*, pp. 142–153, 2023.
- [67] C. Stamouli, L. Lindemann, and G. Pappas, “Recursively feasible shrinking-horizon mpc in dynamic environments with conformal prediction guarantees,” in *Annual Learning for Dynamics & Control Conference*, pp. 1330–1342, PMLR, 2024.
- [68] K. Bestuzheva, M. Besançon, W. Chen, A. Chmiela, T. Donkiewicz, J. van Doornmalen, L. Eifler, O. Gaul, G. Gamrath, A. Gleixner, *et al.*, “Enabling research through the scip optimization suite 8.0,” *ACM Transactions on Mathematical Software*, vol. 49, no. 2, pp. 1–21, 2023.
- [69] M. Vollmer, “Newton’s law of cooling revisited,” *European Journal of Physics*, vol. 30, no. 5, p. 1063, 2009.
- [70] J. Andersson, J. Gillis, G. Horn, J. Rawlings, and M. Diehl, “CasADi: a software framework for nonlinear optimization and optimal control,” *Mathematical Programming Computation*, vol. 11, pp. 1–36, 2019.